4

SYNAPTIC INPUT

How information circulates in the brain was the subject of a heated debate lasting a decade or more among anatomists in the closing years of the last century. One camp argued that neural tissue consisted of a continuum, a *syncytium*, with no discernible functional units while the opposing view held that the brain consisted of discrete units, the nerve cells, communicating through point-to-point contacts that Sherrington dubbed *synapses*. Although in principle both views can be supported, in practice the majority of rapid communication occurs via specific point-to-point contacts, at either chemical and electrical synapses. *Ephaptic transmission* refers to nonsynaptic, electrical interactions between neurons. While such interactions do occur, for instance, among adjacent, parallel axons across the extracellular space, they are, by their very nature, neither very strong among any one pair of processes nor very specific. Their functional significance—if any—is currently not known, and we will not discuss them here (Traub and Miles, 1991; Jefferys, 1995).

In the beginning chapter, we introduced the action of fast, chemical synapses. Given their importance, we will now return to this topic in greater depth. We first overview the pertinent biophysical events underlying chemical synaptic transmission and some of the vital statistics of synapses before we come to the mathematical treatment of synaptic input. In the last section, we will summarize our knowledge of electrical synapses and their computational role.

Most typically, a synapse consists of a *presynaptic* axonal terminal and a *postsynaptic* process that can be located on a dendritic spine, on the trunk of a dendrite, or on the cell body. Figure 4.1 shows some examples of synapses among cortical cells as seen through a high-powered electron microscope. It is not easy at first to identify the synapses amid all the curved, irregular, and densely packed structures making up the neuronal tissue. In a number of locations, such as the retina or the thalamus, a synaptic connection is made between two dendrites, rather than between an axon and a dendrite. These synapses are called *dendrodendritic* synapses; they are believed to be relatively rare in the adult cortex (see Sec. 5.3). Most synapses are small and highly specialized features of the nervous system. As we will see, a chemical synapse converts a presynaptic electrical signal into a chemical signal and back into a postsynaptic electrical signal.

Occasionally, an axon makes a synaptic connection, called an *autapse*, onto its own dendritic tree (van der Loos and Glaser, 1972; Karabelas and Purpura, 1980; Lübke et al.,

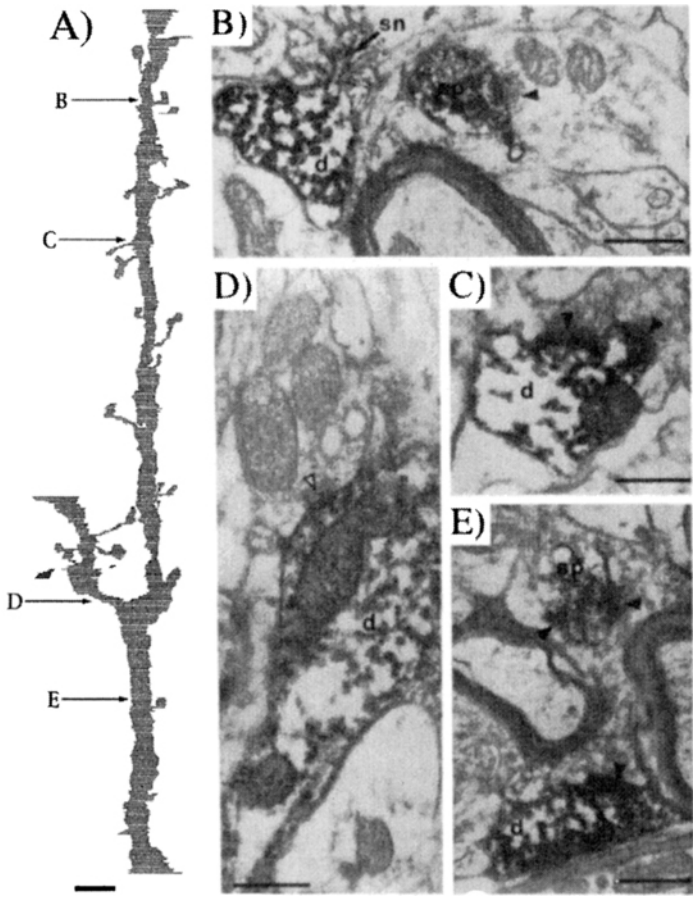

Fig. 4.1 ANATOMY OF CORTICAL SYNAPSES Electron micrographs of spines and synapses on a dendrite of a *spiny stellate* neuron in layer 4 of the visual cortex of an adult cat. Around 300 million synapses are packed into a single cubic millimeter of this tissue, providing the substrate for an extraordinary degree of neuronal interconnectivity. **(A)** 625 ultrathin sections of part of a proximal dendrite of the neuron are shown here in this computer-assisted view. The lower end is close to the soma. The letters and arrows correspond to the electron-microscopic views shown in the adjacent five photographic panels. **(B)** The dendrite (**d**) gives rise to a spine neck (**sn**) and spine head (**sp**). The latter receives an asymmetric, that is, excitatory synaptic profile at the solid arrow. These arrows always point from the unstained presynaptic toward the postsynaptic site. **(C)** Two asymmetric synapses on the dendritic shaft. **(D)** A symmetric, that is, inhibitory synapse (open arrow) at the branch point shown in A. **(E)** A single presynaptic element makes two asymmetric synapses with a spine and a dendrite of the cell. **(F)** An asymmetric synapse with the dendritic shaft. Scale bars equal 2 μm in **A** and 0.5 μm in **B–F**. Reprinted by permission from Anderson et al., (1994).

1996). Autapses appear to be identical to normal chemical synapses. While autapses are rare on pyramidal cells, they are found more frequently on two subclasses of cortical inhibitory interneurons, raising the possibility that they might have a functional role and are not just the unfortunate consequence of an imprecise developmental rule (Tamás, Buhl, and Somogyi, 1997; Bekkers, 1998).

The literature on the properties of synaptic transmission and its molecular nature is gargantuan and keeps growing (Kandel, Schwartz, and Jessell, 1991; Jessell and Kandel,

1993; Stevens, 1993; for a historical overview, see Shepherd, and Erulkar, 1997). We recommend Hille (1992) and Johnston and Wu (1995).

4.1 Neuronal and Synaptic Packing Densities

From the anatomical point of view, synapses in the central nervous system can be conveniently classified according to the detailed morphology of the synaptic profiles in electron-microscopic images into one of two classes, *Gray type I* and *Gray type II* synapses (Gray, 1959). Using a combination of electrophysiological, pharmacological, and anatomical criteria, type I synapses, also known as *asymmetrical synapses*, have been found to be excitatory, while type II synapses, also known as *symmetrical synapses*, act in an inhibitory manner (White, 1989; Braitenberg and Schüz, 1991; Douglas and Martin, 1998; see Fig. 4.1).

Synapses are small. The area of contact between pre- and postsynaptic processes has a diameter of 0.5–1.0 μm, while the presynaptic terminal is only slightly larger. This implies very high synaptic packing densities of around 7.2×10^8 synapses per cubic millimeter in the mouse (Braitenberg and Schüz, 1991). In the cat, the density has been estimated around 3×10^8 per cubic millimeter (Beaulieu and Colonnier, 1985). If the synapses were located on a three-dimensional lattice, they would be spaced a mere 1.1 μm apart. Braitenberg and Schüz (1991) estimate the extent of neuronal processes in a 1-mm^3-cube of cortical tissue, coming up with the staggering amount of 4.1 km total length of axonal processes (at an average diameter of 0.3 μm) and 456 m total length of dendrites (with a diameter of 0.9 μm) in this volume. In other words, the "average" nerve cell in the mouse cortex receives input from 7800 synapses along its 4 mm of dendrites and is connected with 4 cm of "axonal wire" to other cells.

In higher mammals (e.g., mouse, cat, monkey, humans) the total number of neurons in a column of unit area that reaches across all cortical layers is constant, irrespective of what cortical area this column is taken from (the sole exception is the primary visual cortex with 2.5 times more cells). Thus, while the cortical sheet thickened by a factor of 2–3 in its evolution from mouse to human, the number of cells below 1 mm^2 of neocortex remained fixed, in the neighborhood of around 100,000 cells below a square millimeter of cortex (Rockel, Hiorns and Powell, 1980).

Given an approximate density of 100,000 cells per mm^3 in the primate, a synaptic density of 6×10^8 per mm^3, a total surface area of about 100,000 mm^2 for one hemisphere, and an average thickness of about 2 mm, the average human cortex contains on the order of 20 billion neurons and 240 trillion synapses (2.4×10^{14}), quite impressive numbers given the current count of about 10^{11} transistors in the memory and central processing unit (CPU) of a modern parallel supercomputer.[1]

4.2 Synaptic Transmission Is Stochastic

Our view of the synapse is based upon the influential work of Katz and his collaborators (Katz, 1969). Working on the frog neuromuscular junction, they described the basic features

1. Of course, the connectivity among the components in the CPU is three to four orders of magnitude lower than the connectivity of a cortical cell. On the other hand, the cycle time of such machines, in the low nanosecond range, compares very favorably with neuronal time constants in the millisecond range.

of synaptic transmission upon which every further model has been based (Salpeter, 1987). This canonical view is outlined in Fig. 4.2.

The neurotransmitter is prepackaged in numerous small (30–40-nm-diameter) spheres or *vesicles* which reside in the presynaptic terminal. Invasion of the presynaptic axonal terminal by an action potential causes a inrush of calcium ions (via voltage-dependent calcium channels in the presynaptic terminal). These calcium ions—through a complex chain of events—cause one or more synaptic vesicle to fuse with the membrane at special sites. Here, the vesicle now releases its "quantum" of transmitter into the narrow synaptic cleft between the pre- and postsynaptic cell membranes (Fig. 4.2), a process termed *exocytosis*. Calcium is necessary for synaptic transmission. Reducing the extracellular calcium concentration can drastically lower the efficiency of the synapse (Mintz, Sabatini, and Regehr, 1995; Borst and Sakmann, 1996). This might have important functional consequences (Sec. 20.3).

The neurotransmitter rapidly diffuses across the 20-nm-wide *synaptic cleft* and binds to postsynaptic receptors, usually ionic channels. These receptors are then responsible for the great diversity of postsynaptic events that cause the postsynaptic membrane potential to change. Each quantum of transmitter is released probabilistically and independently of the others, and their postsynaptic effects add linearly. One reason for the success of Katz's theory is that its predictions have been evaluated quantitatively (Katz, 1969). If n sites exist, and each such site independently releases either no or only a single packet or quantum of transmitter with an associated amplitude q and with probability p, then the probability of k quanta being released at the entire synapse is given by the binominal distribution

$$p(n, k) = \frac{n!}{(n-k)!k!} p^k (1-p)^{n-k}. \tag{4.1}$$

At the frog's neuromuscular junction, where the theory was developed and the critical experiments were performed, the probability of release can be quite low. Yet because there exist on the order of 100 to 1000 release sites, overall synaptic transmission from the

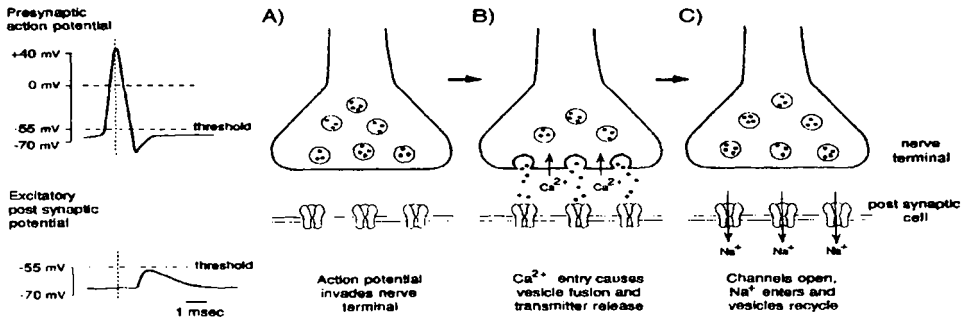

Fig. 4.2 Elements of Synaptic Transmission Standard model of synaptic transmission at a chemical synapse, as elucidated by Katz for the neuromuscular junction. An action potential (far upper left) invades the presynaptic terminal (**A**) and—mediated by the resultant influx of calcium ions—causes the vesicles to fuse with the membrane and release the neurotransmitter inside the vesicle into the synaptic cleft separating the presynaptic membrane from the postsynaptic one (**B**). The neurotransmitter molecules rapidly diffuse across the cleft and bind to the receptors there. In this illustration, they cause the opening of Na^+ selective channels (**C**), leading to an excitatory postsynaptic potential (far bottom left). At central synapses, a similar chain of events occurs, except that the entire process of synaptic transmission appears to be highly stochastic. Reprinted by permission from Jessell and Kandel (1993).

nerve onto the muscle is very reliable. In a somewhat more general version of this model, spontaneous release of vesicles, that is, the spontaneous postsynaptic potentials, can be accounted for by making the probability of release time dependent such that it is very small, but nonzero, in the absence of any input and much larger following a nerve impulse arrival (Katz and Miledi, 1965; Barrett and Stevens, 1972).

While many of the same principles elucidated by Katz also appear to apply to more central synapses, several crucial differences have emerged (Walmsley, Edwards, and Tracey, 1987; Redman, 1990; Stevens, 1993). The most important one concerns the reliability and variability of synaptic transmission. At central synapses, it appears that each synaptic bouton contains only one or a few active release zones, rather than the hundreds found at the neuromuscular junction (Korn and Faber, 1991). In other words, upon arrival of an action potential at an individual anatomically identified synapse, typically none or only one vesicle is released (*one-vesicle hypothesis*; Korn and Faber, 1993). Because only one vesicle is released at each synapse, the probability of release p looms large in whether or not a presynaptic action potential results in a postsynaptic signal.

We know from *in vitro* studies that the probability of release at an individual synapse in vertebrates as well as in invertebrate systems can be highly variable and is usually in the range of between 0.1 to 0.9 (Korn, Faber, and Triller, 1986; Bekkers and Stevens, 1989; Redman, 1990; Edwards, Konnerth, and Sakmann, 1990; Raastad, Storm, and Andersen, 1992; Laurent and Sivaramakrishnan, 1992; Hessler, Shirke and Malinow, 1993; Gulyás et al., 1994).

The molecular origin of the probabilistic release is not yet clear. However, it is likely to relate to the fact that exocytosis depends on a very high local calcium concentration inside the synaptic terminal and that this depends on the vagaries of the exact spatial relationship between calcium channels in the membrane and the location of the vesicle (Borst and Sakmann, 1996; Bennett, 1997).

4.2.1 Probability of Synaptic Release p

Failure of synaptic transmission is vividly demonstrated in Fig. 4.3 (see also Bekkers, Richerson, and Stevens, 1990). Using a so-called minimal stimulation paradigm, only a single Schaffer collateral axon is stimulated. These axons typically make only a single excitatory synapse onto CA1 pyramidal cells (Sorra and Harris, 1993). If the presynaptic-postsynaptic connection were secure, each presynaptic stimulus generated by the electrode should evoke a postsynaptic event. In this case, the membrane potential in the pyramidal cells is clamped to its resting potential and the resultant excitatory postsynaptic current (EPSC) is recorded. The five records in the left column and the four top records in the right column in Fig. 4.3 show nine trials, of which only three lead to a postsynaptic event. The bottom right record corresponds to the average postsynaptic event (averaged over the nine records).

As we will discuss in Chap. 13, the probability of synaptic release p is itself subject to change, depending on the recent history of the presynaptic terminal. Depending on the number and timing of presynaptic action potentials, p can either decrease, as in long-term depression, or increase, as in long-term potentiation. p also varies from one synapse to the next. This behavior might well be different from one synaptic type to the next (e.g., thalamo-cortical versus intracortical synapses; Stratford et al., 1996). Understanding the dynamics of p and its relationship to synaptic plasticity has been a hot research topic of the last few years.

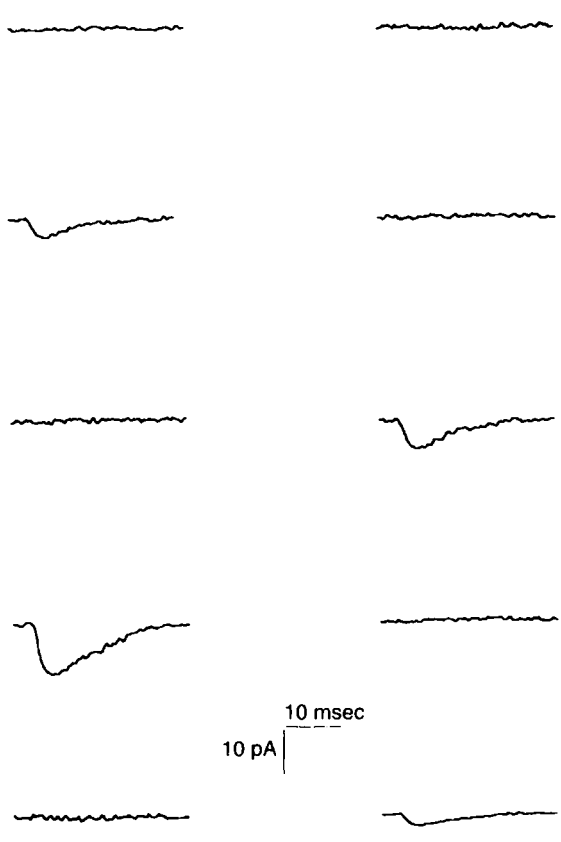

Fig. 4.3 SYNAPTIC TRANSMISSION IS VERY UNRELIABLE Synaptic transmission among central neurons can be highly unreliable and should be thought of as a binary event with a probability of success p, which can be as low as 0.1. This is exemplified by this recording of the excitatory inward current caused by a single synapse, made by a Schaffer collateral axon onto a CA1 pyramidal cell in the mammalian hippocampal slice. The five records on the left and the top four records on the right (30 msec long) show the postsynaptic current in response to nine stimulations of the presynaptic axon using an electrode. Only in three trials does the presynaptic spike lead to the release of a vesicle filled with neurotransmitter that causes a postsynaptic current to flow. The amplitude of this postsynaptic event, if it occurs, is also highly variable. The average postsynaptic EPSC (computed over these nine trials) is indicated on the lower right. It is not clear how the brain deals with the unreliability present at its elementary computational units. Unpublished data from Y. Wang and C. Stevens, printed with permission.

In the example of Fig. 4.3, the probability of release is about 0.3. This is quite remarkable, since it implies that the connecting elements among neurons are binary but highly unreliable circuit elements, transmitting only one out of three events. Imagine a transistor that only conducts, that is, switches, one out of three times that a charge is dumped onto its gate. Synapses made onto pyramidal cells in slices from sensory and motor cortex appear to behave in an identical fashion (Smetters and Nelson, 1993; Thompson, Deuchars, and West, 1993a,b). An important *caveat* is that these results were not obtained under physiological conditions in intact animals but in slices or other isolated preparations. It is possible that in a behaving animal, various neuromodulators can significantly boost or reduce p.

The lack of reliability of synapses should be compared to a reliability of transmission among electronic circuits, which is many, many orders of magnitude higher.[2] In principle, the nervous system could compensate for such unreliable components by exploiting redundancy (Moore and Shannon, 1956; von Neumann, 1956), that is, by using many parallel synapses. Yet, it is common for a cortical axon to make only one or two synaptic contacts onto its target cell (Gulyás et al., 1993; Sorra and Harris, 1993). The brain must have found a different way in which it deals with such unreliable synaptic components.

The reliability of synaptic transmission in the central nervous system is further compromised by the fact that the variability in the amplitude of the postsynaptic response to the release of a single packet of neurotransmitters is much larger than at peripheral synapses. Thus, even if a packet of neurotransmitters is released, a number of factors, such as the variation in the size of the vesicle and the number of postsynaptic receptors, cause the postsynaptic response to this presynaptic event to vary from one trial to the next (see the three successful instances of transmission in Fig. 4.3; Bekkers, Richerson, and Stevens, 1990; Larkman, Stratford, and Jack, 1991). In the study by Mason, Nicoll, and Stratford (1991), the variance in the size of the EPSP—evoked in one rat neocortical pyramidal cell by electrically activating a nearby pyramidal cell —is as large as its mean (Fig. 4.4), with the largest EPSP (2.08 mV) about 40 times larger than the smallest (0.05 mV). In these experiments, the number of synapses between the pair of cells recorded from is not known (see also Stratford et al., 1996).

We defer a discussion of the possible functional role of the stochastic nature of synaptic transmission to Sec. 13.5.5.

4.2.2 What Is the Synaptic Weight?

Let us briefly address the thorny issue of what exactly constitutes *synaptic weight* or *synaptic strength*. In the neural network literature, this is a single scalar, usually labeled w_{ij} or T_{ij} (see Sec. 14.4). However, synapses are very complicated devices, which are characterized by numerous parameters. Traditionally—as expressed by Eq. 4.1—biophysicists have used three scalar variables to describe a synapse: the number of quantal release sites n, the probability of synaptic release per site p, some measure of the postsynaptic effect of the synapse q. Depending on the experiment, q can be the peak conductance, the maximal synaptic current at some potential, or the peak EPSP. Of course, in real life, n is drawn from some probability distribution (usually binominal or Poisson), p depends on the previous spiking history, and q itself is a function of time (such as the time-dependent conductance change of Eq. 1.21).

One possible relationship between these state-dependent functions and the synaptic weight is the expected or mean postsynaptic action, computed by averaging over a Poisson distributed presynaptic spike distribution with

$$R = npq\,. \tag{4.2}$$

We shall return to this in Chap. 13. However, one should never forget that the averaging assumptions used to compute this weight might not be relevant to the brain under its normal operating conditions (for instance, since the input is oscillatory or tends to fire in bursts or because its stochastic nature is critical).

2. Indeed, in digital CMOS technology, where the signal gain at an inverter, the elementary computational unit, is in the neighborhood of 15 to 20, the thermal fluctuations—on the order of 0.65 mV at room temperatures—are so much less than the switching voltage, that the probability of switching is about $1 - 10^{-14}$. Given that each inverter restores the input signal, the effect of thermal noise does not accumulate along a cascade of inverters.

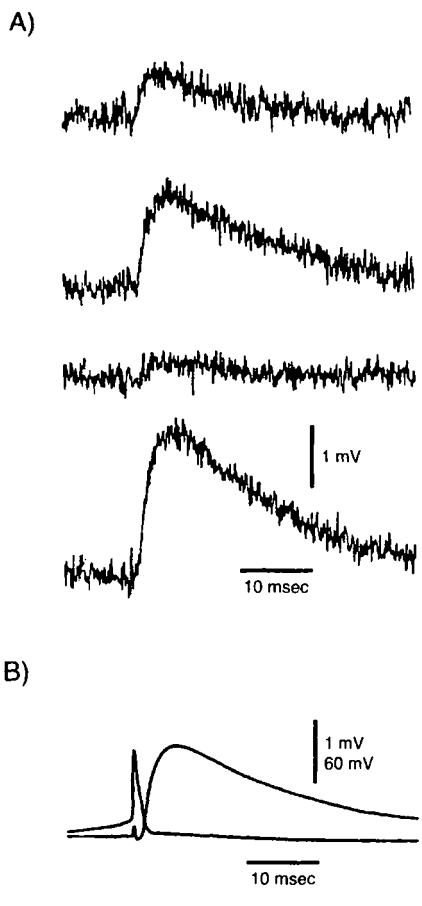

Fig. 4.4 Postsynaptic Amplitude Is Highly Variable Fluctuations in the amplitude of EPSPs observed in a pyramidal cell by evoking an action potential in a nearby pyramidal cell. Both pairs of neurons are located in layer 2/3 of brain slices taken from rat visual cortex. **(A)** Four individual sweeps from the same synaptic connection. The EPSP amplitude over the entire population of cell pairs is 0.55 ± 0.49 mV. **(B)** Average of 2008 such sweeps, together with the presynaptic record, showing that the EPSP in the postsynaptic cell is caused by the presynaptic spike. Due to technical reasons, no events less than 0.03 mV—and, in particular, no failures as in Fig. 4.3—can be recorded. Reprinted by permission from Mason, Nicoll, and Stratford (1991).

In summary, because of the highly probabilistic nature of the release of neurotransmitter, compounded by the variability in the size of the postsynaptic responses to this neurotransmitter, a basic and unavoidable feature of interneuronal communications using chemical synapses is their lack of reliability and consistency. As pointed out by Stevens (1994), it is crucial that any theory of the brain account for this fundamental property of neuronal hardware. We will return to the theme of stochastic computations in the brain in Chap. 15.

4.3 Neurotransmitters

The plethora of time courses, amplitudes, and types of actions seen in synaptic transmission is the result of the interplay between different *neurotransmitters*, stored in vesicles at the presynaptic terminal, and different synaptic *receptors*, inserted in the postsynaptic membrane.

There exist three major chemical classes of neurotransmitters, *amino acids, biogenic amines,* and *neuropeptides* (Table 4.1). Fast synaptic transmission in the central nervous

system of vertebrates is mainly mediated by amino acids, the major excitatory neurotransmitters being *glutamate* and *aspartate*, and the major inhibitory neurotransmitters being γ-amino-butyric acid (GABA) and *glycine*. The onset of the associated excitatory or inhibitory postsynaptic currents (EPSCs or IPSCs), forming the principal substrate of neural computation, is rapid (<1 msec) and their durations are relatively short (<20 msec). All these neurotransmitters also have slow effects.

The list of biogenic amines that can modulate the response of the cell to synaptic input includes *acetylcholine* (ACh), *norepinephrine* (also referred to as *noradrenaline*), *dopamine, serotonin* and *histamine*. Usually, their actions have a much slower onset than the action of amino acids and may persist hundreds of milliseconds to seconds. However, some neuroactive substances, such as acetylcholine, cause fast (e.g., nicotinic-receptor-mediated fast synaptic transmission at the vertebrate neuromuscular junction) as well as slow (e.g., muscarinic-receptor-mediated changes in potassium conductances) effects, depending on which receptor is present in the postsynaptic membrane.

A long and ever-growing list of *peptides*, that is, short chains of amino acids, modulates the response of neurons over very long time scales (that is, minutes). *Hormones*, that is substances that are transported via the bloodstream (in vertebrates) or the hemolymph (in invertebrates), also affect neuronal responses, with the distinction between the actions of neuropeptides and hormones being a gradual one. These neuroactive substances, frequently also termed *neuromodulators*, are usually *colocalized* with conventional fast neurotransmitters in individual neurons. Indeed, sometimes two or more neuropeptides can be colocalized within a conventional terminal in different vesicles (Kupfermann, 1991). Release can be differential, in the sense that the release of the vesicles containing the modulators requires a higher presynaptic firing rate than release of the vesicles harboring the fast neurotransmitter. Dozens of peptides and hormones have been identified in small invertebrate ganglia that are accessible to neurochemical methods (Marder, Christie, and Kilman, 1995; see also Fig. 20.5), and it is unlikely that the situation in the cortex will be much simpler.

The concentration of these substances can be thought of as the closest equivalent to a *global variable* in the brain. While a global variable within a computer program is defined for the entire program (rather than for any particular procedure), similarly, release of a long-lasting neuromodulatory substance will affect all neurons within a given distance from the site of release. As we will see in the next section, neurons possess receptors for a variety of different neurotransmitters and modulators, giving rise to a very complex and possibly redundant system for modulating the electrical responses of neurons over a great variety

TABLE 4.1
Principal Neurotransmitters

Amino acids	Biogenic amines	Neuropeptides
Glutamate	ACh	Substance P
Aspartate	Dopamine	Somatostatin
GABA	Noradrenaline	Proctolin
Glycine	Serotonin	Neurotensin
	Histamine	Luteinizing-hormone-releasing hormone (LHRH)

Three main chemical classes of neurotransmitters found in the nervous systems of all animals. Amino acids are usually involved in fast (glutamate/aspartate) excitatory or inhibitory (GABA/glycine) synaptic traffic. Many substances, such as glutamate or acetylcholine (ACh), have fast and transient as well as slow and long-lasting effects, depending on the postsynaptic receptor. The very large number of *neuropeptides*, of which only a handful are listed, act on the time scale of seconds to minutes.

of different spatial and temporal scales (for reviews see Nicoll, 1988; Kupfermann, 1991; Hille, 1992; Bourne and Nicoll, 1993; McCormick, 1998). This implies that cells can be "addressed" using a unique bar-code-like combination of neuromodulators and receptors (see Sec. 20.5).

4.4 Synaptic Receptors

Postsynaptic receptors come in two different flavors (Fig. 4.5). *Ionotropic* receptors are directly coupled to ionic channels, which open and permit certain types of ions to cross the postsynaptic membrane. Such channels, also called *ligand-gated* channels, include the *nicotinic* acetylcholine receptor in the peripheral nervous system of vertebrates and many invertebrates, the $GABA_A$ receptor complex, and the ubiquitous glutamate *N*-methyl-D-aspartate (NMDA) and non-NMDA channel complexes (Table 4.2). Given the close point-to-point connection between the presynaptic release zone and the postsynaptic receptor (Fig. 4.1) and the direct coupling between the receptor and the channel (Figs. 4.2

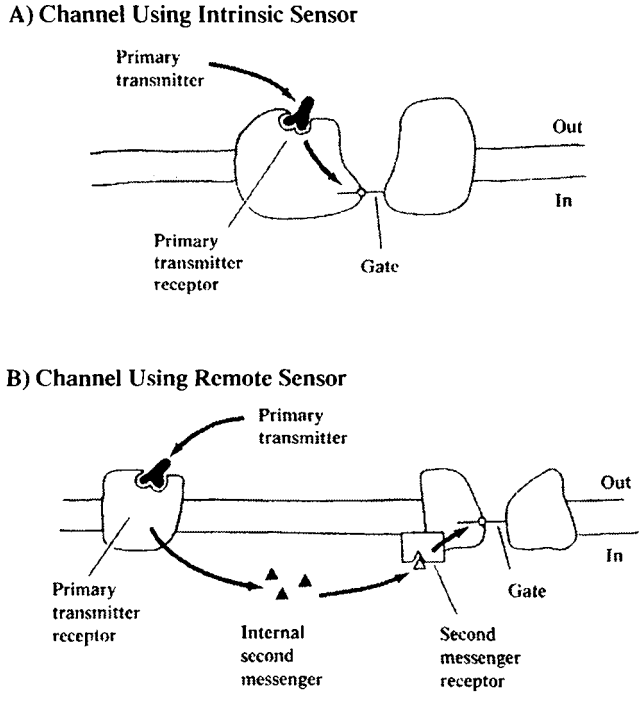

Fig. 4.5 IONOTROPIC AND METABOTROPIC SYNAPTIC ACTION **(A)** Fast excitatory and inhibitory input mediated by a tightly linked *ionotropic* receptor-channel complex. Binding of the neurotransmitter leads to a rapid opening of the associated ionic channel. **(B)** In the case of a *metabotropic* receptor, binding of the neurotransmitter leads to activation of a second messenger substance (such as Ca^{2+} ions). This messenger molecule, possibly after diffusing to its site of action, binds to a particular ionic channel and will modulate its properties. While the action of the ionotropic receptor is point to point and rapid, both the onset and the duration of the metabotropic mediated synaptic input are usually slow and its action can extend over larger distances. Both receptor types can be colocalized. Reprinted by permission from Hille (1992).

TABLE 4.2
Synaptic Receptor Types

Neurotransmitter	Receptor	E_{syn}	Type	Comments
Glutamate	Non-NMDA	0	I	Very fast
Glutamate	NMDA	0	I	Voltage dependent
GABA	$GABA_A$	−70	I	Fast inhibition
GABA	$GABA_B$	−100	M	Slow inhibition
ACh	Nicotinic	−5	I	Neuromuscular junction
ACh	Muscarinic	−90	M	Decreases K conductance
Noradrenaline	α_2	−100	M	Increases K conductance
Noradrenaline	β_1	−100	M	Decreases K conductance

List of major types of synaptic receptors and the associated neurotransmitters. The four top listings are the dominant transmitters used for fast communication in the vertebrate central nervous system. The synaptic reversal potential E_{syn} is specified in millivolts absolute potential. The type corresponds to either ionotropic (I) or metabotropic (M) receptors.

and 4.5A), the action of ionotropic receptors is rapid and transient. They implement the computations underlying rapid perception and motor control.

Binding of neurotransmitter to *metabotropic* receptors, on the other hand, leads to the activation of some intracellular molecules, termed *second messengers*, which in turn may induce a conformational change in some ionic channel and therefore in its kinetic behavior.

It has been estimated that the mammalian genome has devoted about 1000 of its 10^5 genes to these receptors. They could encode for a truly staggering number of different metabotropic receptors. At the molecular level, all of these receptors span the cell membrane in a snakelike fashion, crossing the bilipid membrane seven times (Chap. 8). These receptors connect with so-called *G proteins* just inside the cell membrane. G proteins, named because they bind guanosine triphosphate (GTP), include at least 20 different proteins and are among the most versatile nanomachines in biology (Clapham, 1996). Acting on perhaps 100 different receptors throughout the brain, the muscles, the glands, and other organs, they recognize photons (rhodopsin) and odor molecules as well as conventional neurotransmitters, such as glutamate, GABA, and ACh (Ross, 1989; Hille, 1992). Activation of these receptors is linked via a cascade of biochemical reactions to the ionic channel that is modulated (Fig. 4.5B). Functionally, these multiple intracellular steps can greatly amplify the signal. Thus, a single occupied receptor might activate many G proteins, each one of which can, in turn, activate many other proteins, and so on. Second messengers can act to increase or to decrease the postsynaptic membrane conductance, in particular for potassium.

An important distinction between ionotropic and metabotropic receptors is their time scale. While members of the former class act rapidly, terminating within a very small fraction of a second, the speed of the latter class is limited by diffusion. Biochemical reactions can happen nearly instantaneously at the neuronal time scale. However, if a synaptic input to a metabotropic receptor induces the release of some messenger, such as calcium ions, which have to diffuse to the cell body in order to "do their thing," the time scale is extended to seconds or longer. Section 9.3 details the involvement of one such metabotropic receptor type in the control of firing frequency adaptation.

It is difficult to overemphasize the importance of modulatory effects involving complex intracellular biochemical pathways. The sound of stealthy footsteps at night can set our heart to pound, sweat to be released, and all our senses to be at a maximum level of alertness,

all actions that are caused by second messengers. They underlie the difference in sleep-wake behavior, in affective moods, and in arousal, and they mediate the induction of long-term memories. It is difficult to conceptualize what this amazing adaptability of neuronal hardware implies in terms of the dominant Turing machine paradigm of computation.

Because of the indirect coupling between receptor and effector—in particular if the second messengers involved have to diffuse within the postsynaptic cell—the onset of their effects is usually slow but long-lasting and is not restricted to a single site. They modulate the properties of groups of neurons over long time scales, that is, hundreds of milliseconds to seconds, minutes, and longer. Yet, this view does not do justice to the overlapping time scales of ionotropic and metabotropic receptors. If receptor and effector are spatially close to each other, both can act at the same time scale. For instance, a ligand-gated event such as a glutamate-induced NMDA depolarization lasts for 50–100 msec, approximately the same duration as a second-messenger-mediated hyperpolarization caused by activation of $GABA_B$ receptors.

4.5 Synaptic Input as Conductance Change

Activation of an ionotropic receptor permits the associated ionic channel in the postsynaptic channel to change its configuration, thereby allowing the passage of ions across the membrane. Given the small diameter of the open channel, about 3-7 Å, channels are highly selective for certain ions that diffuse through the open channel down their electrochemical gradient, leading to a change in postsynaptic potential. Chapter 8 will treat ionic channels in more detail. At this point, all we need to know is that individual channels act as binary elements, having zero conductance in their closed state and a fixed, nonzero conductance value in their open state (ranging between 5 and 50 pS, depending on the channel type).[3] The graded nature of the observed postsynaptic conductance change comes from the simultaneous openings of tens to hundreds of these binary elements. How long these channels stay open—the determinant of the duration of synaptic input—depends on two factors: (1) the presence of active uptake systems in the synaptic cleft that can remove the neurotransmitter and degrade or recycle it, and (2) the internal kinetics of the channel.

4.5.1 Synaptic Reversal Potential in Series with an Increase in Conductance

Given the distribution of ions in the intracellular and extracellular cytoplasm and the specificity of the ionic channels, each type of synaptic input has an associated *Nernst potential*, also referred to as the *ionic battery*, or *ionic reversal potential*, E_{syn}. The origin of this potential—crucial to neuronal excitability— relates to the equilibrium established between the concentration gradient of the different ions across the neuronal membrane and the electrical force opposing this gradient. Using the Boltzmann equation of classical statistical mechanics, the value of the synaptic potential at body temperature for a channel permeable to a single ionic species is given by the Nernst equation

$$E_{syn} = \frac{61.5}{z} \log_{10} \frac{[S]_o}{[S]_i} \tag{4.3}$$

where E_{syn} is measured in millivolts, z is the valence of the ions involved (positive for Ca^{2+}, Na^+ and K^+ ions, negative for Cl^- ions) and $[S]_o$ is the extra- and $[S]_i$ the

3. We here neglect the fact that many channels have more than one open state; this is usually described by saying that a channel has conductance *sublevels*.

intracellular concentration of the ionic species considered. The meaning of E_{syn} becomes clearer if one considers that in the absence of any other ionic species, the membrane potential across the open channel would stabilize at E_{syn}. At this potential, the ions on both sides of the membrane are in a dynamic equilibrium, with no net flux of ions through the channel. Many channels are permeable to a mixture of two or more ionic species, requiring a more complex expression, such as the *Goldman-Hodgkin-Katz* (GHK) *voltage equation* (Goldman, 1943; Hodgkin and Katz, 1949; Hille, 1992).

As we saw in the first chapter, the opening of a synaptic channel corresponds, from an electrical point of view, to an increase in the membrane conductance in series with the ionic reversal battery E_{syn} (Fig. 1.7A). The key insight, namely that the binding of neurotransmitters causes an increase in the *conductance* of the membrane, came from research carried out by Fatt, Katz, and Eccles in the 1950s as they were working on the neuromuscular junction (Eccles, 1964, 1990).

The lumped effect of many ionic channels opening in response to the binding of the transmitter molecules to the receptor is treated as a time-varying change in the membrane conductance $g_{syn}(t)$ in series with the synaptic reversal potential E_{syn}. This conductance change gives rise to a transient ionic current through the open channels, transporting charge across the membrane. How does the synaptic current relate to the conductance of the channel and to the membrane potential?

In general, this relationship is a complex one. One such description is referred to as the *Goldman-Hodgkin-Katz current equation* (Goldman, 1943; Hodgkin and Katz, 1949; Hille, 1992; see Eq. 9.1). Assuming that ions cross the membrane without interacting with each other and that the potential drops linearly across the membrane, the GHK current equation expresses a nonlinear dependency between the ionic current and the membrane voltage. This nonlinearity, referred to as *rectification* since current passes more easily in one direction than in the other, is caused by the nonhomogeneous distribution of ions across the membrane and increases with increasing concentration gradient.

However, in general, a linear relationship is observed between synaptic current and the membrane potential (with the important exception of the NMDA receptor discussed below). In fact, once the reversal potential has been accounted for, *Ohm's law* appears as a satisfactory first-order description of the synaptic current, and this is the one we adopted at the beginning of this book (e.g., Eq. 1.18),

$$I_{syn}(t) = g_{syn}(t)(V_m(t) - E_{syn}) \tag{4.4}$$

It is important to realize that the synaptic current depends on V_m. Only under certain conditions can a synaptic input be approximated as a constant current source (Fig. 1.7B). This seemingly trivial observation has a number of important consequences, outlined further below as well as in Chaps. 5 and 18. Equation 4.4 is a purely phenomenological description of the current as a function of the membrane potential and is not derived from first principles. Experimentally, linearity is not necessarily assured and needs to be experimentally confirmed (as, for instance, in Hestrin et al., 1990a, for the fast, non-NMDA input onto hippocampal pyramidal cells).

A synapse is excitatory if the synaptic current I_{syn} depolarizes the postsynaptic membrane by giving rise to an EPSP. Activation of an inhibitory synapse, on the other hand, can either clamp the potential to remain around V_{rest} or cause an outward current to flow, thereby giving rise to an IPSP that hyperpolarizes the cell. In the language of the electrophysiologist, an excitatory synapse injects current into the cell; such inward currents are represented, by convention, as negative currents. For synapses with $g_{syn} \geq 0$, an excitatory synapse has a

reversal potential more positive than the resting potential, while an inhibitory synapse has a reversal potential close to or negative to the resting potential.[4]

Figure 4.6 illustrates the typical sequence of a fast EPSP followed by a fast and a slow IPSP seen in a cortical pyramidal cell upon electrical stimulation of the fibers projecting into cortex. The hyperpolarizing potentials are caused by inhibition acting on two separate inhibitory receptors ($GABA_A$ and $GABA_B$) discussed further below.

4.5.2 Conductance Decreasing Synapses

In general, the release of neurotransmitters at an ionotropic synapse increases the postsynaptic membrane conductance, that is, $g_{syn}(t) > 0$. At metabotropic receptors, this need not be the case. A well-known example is the loss of firing rate adaptation seen in hippocampal neurons following the stimulation of fibers releasing noradrenaline. This input leads to the reduction of a calcium-dependent potassium conductance (Fig. 9.9). Another example is the change occurring in the responsivity of thalamic relay cells when mammals wake

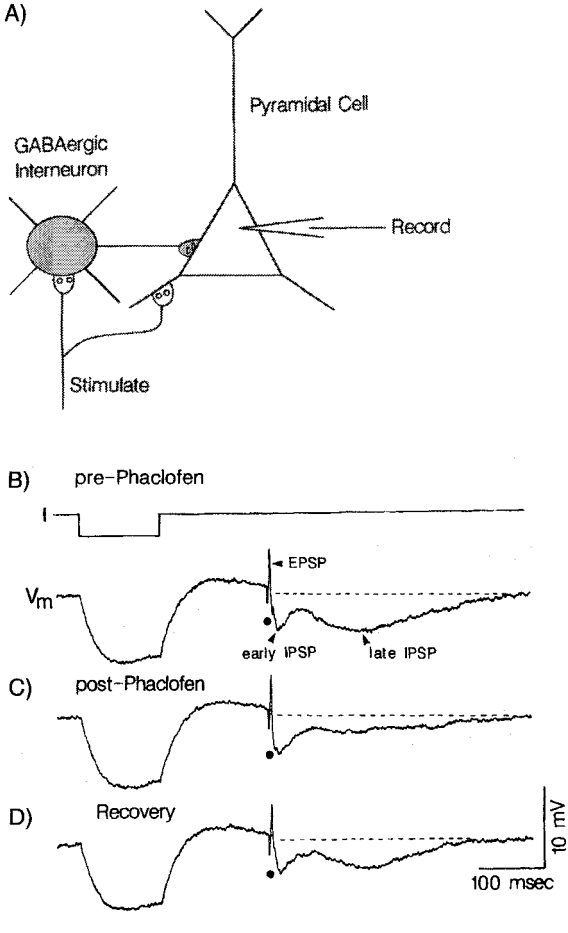

Fig. 4.6 SYNAPTIC POTENTIALS GENERATED IN A CORTICAL CELL **(A)** Electrical stimulation of axons ascending into the cerebral cortex generates a very rapid EPSP, terminating within 10 msec, followed by two IPSPs, an early fast one and a late slow one. This sequence of events is common to most cortical cells upon stimulation of their extracortical afferents (Douglas, Martin, and Whitteridge, 1991; Tseng and Haberly, 1988). **(B)** and **(D)** The inhibition is caused by recruitment of cortical interneurons, which release GABA acting on two distinct synaptic receptors. The early IPSP is due to activation of the ionotropic $GABA_A$ receptors, causing an increase in a chloride membrane conductance, while the late IPSP is due to $GABA_B$ receptor activation. This metabotropic synapse causes a hyperpolarizing potassium conductance to open. **(C)** Applying the substance phaclofen to the slice blocks the $GABA_B$ receptors while not affecting the $GABA_A$-mediated IPSP. The constant current pulse at the beginning of the trace (see B) assesses the extent to which the input resistance changes during application of phaclofen (it does not). Reprinted by permission from McCormick (1998).

4. However, under certain circumstances inhibitory input can act functionally as if it were exciting a cell and vice versa (Lytton and Sejnowski, 1991).

up (that is, the switch from slow-wave sleep to awake, attentive state). Activation of a variety of different metabotropic receptors (e.g., muscarinic ACh receptors, receptors for adrenaline and histamine; McCormick, 1992) causes a 10-mV or greater increase in the resting potential. This sustained depolarization, triggered by the *reduction* of a potassium "leak" conductance (that is, $g < 0$), is sufficient to switch the cell from a bursting into a single action potential firing mode with important consequences for information processing (Steriade and McCarley, 1990; McCormick, 1992).

In summary, the postsynaptic effect of a chemical synapse involves a transient change $g_{syn}(t)$ in the membrane conductance in series with a synaptic battery E_{syn}. Before we discuss the biophysical consequences of this further, let us summarize the key properties of the most common forms of excitatory and inhibitory synaptic input.

4.6 Excitatory NMDA and Non-NMDA Synaptic Input

The predominant fast, excitatory neurotransmitter of the vertebrate central nervous system is the amino acid *glutamate*, activating synaptic receptor channels on nearly every nerve cell as well as on many of the supporting glia cells. In the peripheral nervous system of vertebrates, glutamate synapses are nearly unknown. Here the dominant fast neurotransmitter is ACh. Invertebrates use ACh as well as glutamate for fast transmission of information throughout their nervous systems.

Applying glutamate or its close relative *aspartate* onto central neurons causes a fast depolarizing event, providing the substrate for the fast excitatory traffic in the central nervous system. However, receptors sensitive to glutamate turn out to be a diverse lot and their various subtypes are now being expressed using molecular techniques (Sommer and Seeburg, 1992; Westbrook, 1994). About two dozen glutamate receptor subunits have been cloned from the rat brain, some of which are ionotropic and some metabotropic receptors (Dingledine and Bennett, 1995). These are expressed in different locations throughout the brain and differ in their kinetics, degree of voltage dependency, and so on. Thus, quite different from commercial analog and digital CMOS highly integrated silicon circuits, where the degree of specialization of transistors and circuit types across the chip is minimal, each circuit in an animal may use a slightly different synaptic subtype (possibly also depending on the history of the animal as well as on its developmental stage).

The study of glutamate receptors and their associated synaptic properties is currently in a very active phase. We summarize here the pertinent facts of this unfolding story (Ascher and Nowak, 1988; Thomson, Girdlestone, and West, 1988; Bekkers and Stevens, 1989; Hestrin et al., 1990a,b; Mason, Nicoll, and Stratford, 1991; Williams and Johnston, 1991; Stern, Edwards, and Sakmann, 1992; Jonas and Spruston, 1994; Destexhe, Mainen, and Sejnowski, 1994a).

The most important distinction among excitatory glutamate synapses is based on applying various pharmacological substances to the receptor and measuring their action. One set of these agents, called generically *agonists*, activates one subclass of glutamate receptors, with different chemical substances binding to different receptors, like keys fitting into locks. The different receptors are usually identified by the name of their agonists.

In the case of the glutamate-sensitive receptor, two major functional subclasses exist (as mentioned above, many more molecular subtypes have been cloned, but their specific functions are not yet known). One receptor binds kainate, quisqualate, and α-amino-3-hydroxy-5-methyl-4-isoxalone propionic acid (AMPA). The other class of glutamate

receptors can be selectively activated by NMDA. In other words, dumping NMDA onto the synapse causes it to bind to the NMDA receptor and the associated synapse to open. It is important to realize that NMDA, AMPA, and the other agonists do not exist within the nervous system but are pharmacological substances used by biophysicists to identify the receptors. In the brain, all glutamate synapses, regardless of their receptor types, are activated by the presynaptic release of glutamate. Because we are not interested in the various subtypes and the proper nomenclature is still being debated, we simply refer throughout this book to NMDA and non-NMDA synapses.

Other pharmacological agents, so-called *antagonists*, very specifically block the various subclasses of glutamate receptors, allowing us to isolate the contributions of the non-NMDA and the NMDA receptors to EPSPs. For instance, the substance 6-cyano-7-nitroquinoxaline-2,3-dione (CNQX) blocks the fast, non-NMDA synapse without interfering with the NMDA synapse, while DL-2-amino-5-phosphono-valeric acid (APV) blocks the slower NMDA component without blocking the non-NMDA component. Again, antagonists do not occur naturally in the brain but are used as a tool to investigate synaptic transmission.

Once glutamate binds to the AMPA receptor the associated channel opens, allowing monovalent cations, mainly Na^+ and K^+, to flow across the membrane. The synaptic reversal potential of this synapse is about 0 mV (absolute potential). At a non-NMDA receptor, the postsynaptic channels activate very rapidly. The synaptic current peaks within a few hundred microseconds, with an exponential decay whose time constant varies between 0.5 and 3 msec (Hestrin, Sah, and Nicoll, 1990b; Hestrin, 1992; Trussel, Zhang, and Raman, 1993; Jonas, Major, and Sakmann, 1993).

The time course of the synaptic conductance increase can in general be described by an nth-state Markov process with $n(n-1)$ time constants (Destexhe, Mainen, and Sejnowski, 1994a; Johnston and Wu, 1995). Although efficient implementations for these schemes are known (Destexhe, Mainen and Sejnowksi, 1994b), in general simplified expressions are used, the most common being the α function of Eq. 1.21 (Rall, 1967; Jack, Noble, and Tsien, 1975),

$$g_{\text{syn}}(t) = \text{const} \cdot t e^{-t/t_{\text{peak}}} . \tag{4.5}$$

The constant is chosen such that $g_{\text{syn}}(t_{\text{peak}}) = g_{\text{peak}}$, that is, const $= g_{\text{peak}} e / t_{\text{peak}}$. The function $g(t)$ decays to 1% of its peak value at about $t = 7.64 t_{\text{peak}}$. Using $t_{\text{peak}} = 0.5$ msec with a conductance change of between 0.25 and 1 nS reproduces well the observed time course of the non-NMDA input (Fig. 4.7).

Different from the non-NMDA receptor, with whom it usually appears to be colocalized, the amplitude of the conductance change associated with the NMDA synapse depends on the membrane potential. Figures 4.8A and 4.9A illustrate the nonlinear instantaneous I–V relationship. What is apparent is the negative slope-conductance region between -70 and -40 mV. This negative slope is conferred upon the NMDA current by the action of Mg^{2+} ions, which are naturally present in the extracellular environment. If the postsynaptic potential is at rest and glutamate is bound to the NMDA receptor, the channel opens but is physically obstructed by Mg^{2+} ions. As the membrane is depolarized, the Mg^{2+} ions move out, and the channel becomes permeable for a mixture of Na^+, K^+ and a small number of Ca^{2+} ions. The fraction of the current carried by Ca^{2+} ions through the NMDA channel is about 7% (at negative potentials), five times the fractional calcium current through the voltage-independent glutamate channel (Schneggenburger et al., 1993). If the Mg^{2+} ions are removed from the saline solution bathing the neurons in an experimental slice setup, the synapse looses its nonlinearity and becomes purely ohmic (solid line in Fig. 4.8A). The synapse has a reversal potential close to zero. Another difference compared to the

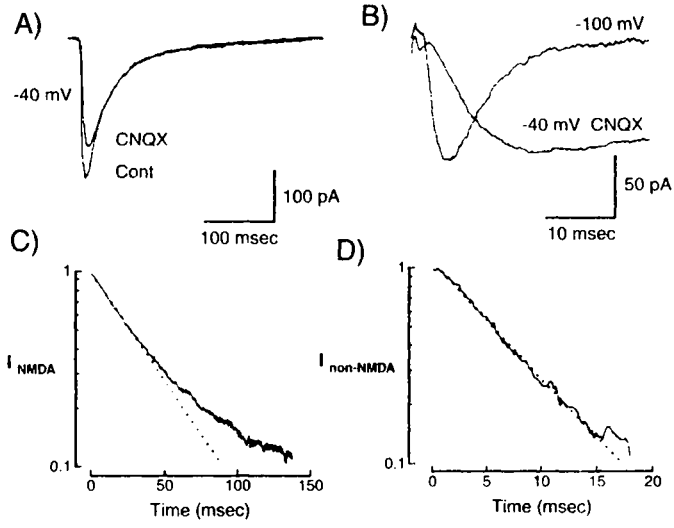

Fig. 4.7 Time Course of Excitatory Synaptic Input Time course of the non-NMDA and NMDA excitatory inputs recorded from cells in hippocampal slices. **(A)** The excitatory postsynaptic current, obtained by clamping the cell to −40 mV and applying glutamate, is shown in the absence (Cont) and presence of the non-NMDA channel blocker CNQX. The remaining current is mediated via NMDA receptors. By convention, depolarizing inward currents are represented as negative currents. **(B)** Closeup of the time course of the NMDA current (labeled CNQX) and the non-NMDA current, obtained by clamping the EPSC to −100 mV and thereby blocking all NMDA channels. The NMDA component continues to rise as the non-NMDA component has started to decay already. **(C)** A semilogarithmic plot of the NMDA-mediated current demonstrates that the decay of the NMDA current is not well fitted by a single exponential (at 31° C). **(D)** The decay of the non-NMDA current (from the curve labeled "−100 mV" in B) is well fitted by a single exponential with a time constant of 7.2 msec (at 24° C). Reprinted by permission from Hestrin, Sah, and Nicoll (1990b)

non-NMDA input is the much slower time course of the NMDA-mediated conductance change due to the intrinsic kinetics of the receptor. Both rise and decay times are at least a factor of 10 times slower, with rise times on the order of 10 msec. Indeed, maximum NMDA receptor activation occurs when the non-NMDA conductance change has almost subsided (Fig. 4.7C).

The NMDA conductance can be derived from a model in which the binding rate constant of Mg^{2+} varies as an exponential function of voltage (Ascher and Nowak, 1988; Jahr and Stevens, 1990). Modeling the time dependency by the difference between two exponentials, we have

$$g_{\text{syn}}(t) = g_n \frac{e^{-t/\tau_1} - e^{-t/\tau_2}}{1 + \eta[\text{Mg}^{2+}]e^{-\gamma V_m}}, \tag{4.6}$$

with $\tau_1 = 80$ and $\tau_2 = 0.67$ msec, $\eta = 0.33/\text{m}M$, $\gamma = 0.06/\text{mV}$ and $g_n \approx 0.2$ to 0.4 nS (at 35° C). The physiological concentration of Mg^{2+} ions is around 1 mM.

The synaptic current is obtained by multiplying this conductance by the membrane potential (since the associated $E_{\text{syn}} \approx 0$). Figure 4.8B shows the time course of an experimentally measured NMDA current as compared with this model.[5] Better fits can be obtained by using more complex models (Clements and Westbrook, 1991).

5. The temperature at which electrophysiological experiments occur has a significant impact on the dynamics of neuronal processes. Experiments on brain slices and cultured neurons are generally carried out around 22–25° C, significantly below the

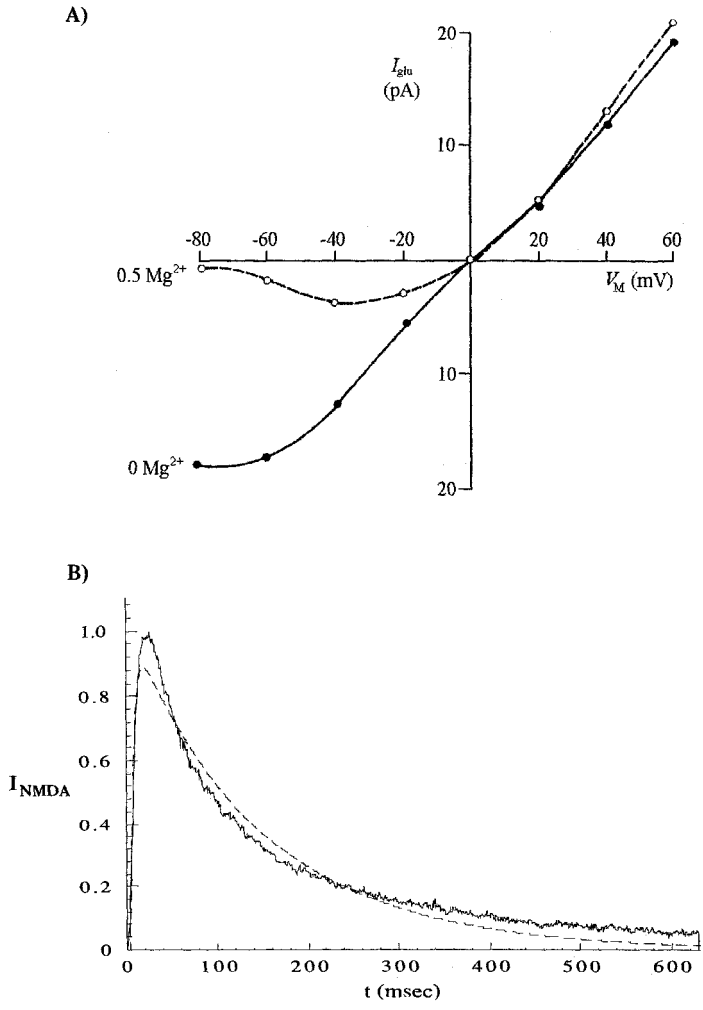

Fig. 4.8 VOLTAGE DEPENDENCY OF THE NMDA CURRENT Current-voltage relationship associated with the NMDA receptor. Because of the action of Mg^{2+} ions in blocking the underlying channel, the associated postsynaptic conductance increase is voltage dependent, different from other fast synaptic inputs. **(A)** Current-voltage relationship of the NMDA current in the absence and presence of 0.5 mM magnesium. While the current behaves relatively ohmic in the absence of magnesium, under physiological concentrations of Mg^{2+} a strong voltage dependency is revealed. Reprinted by permission from Nowak et al. (1984). **(B)** Experimentally recorded normalized NMDA current in a brain slice kept at room temperature (Hessler, Shirke, and Malinow, 1993; heavy jagged line). Superimposed is the current computed from Eq. 4.6, with $\tau_1 = 145.5$ and $\tau_2 = 4.1$ msec. Unpublished data from A. Destexhe, printed with permission.

(continued) 37° C baseline in mammals. In general, the absolute conductances associated with ionic channels vary little with the temperature. However, the rates with which these channels change conformation (Chap. 8) speed up considerably at higher temperatures. The extent of this sensitivity is characterized by the *temperature coefficient* Q_{10}, defined as the increase in rate as the temperature changes by 10° C. Hestrin, Sah, and Nicoll (1990b) report an average temperature coefficient associated with the decay time constant of the fast non-NMDA current of $Q_{10} = 2.7 \pm 0.8$, with a decay equal to 7.9 msec at 26.5° C. This implies a much faster decay of $7.9\ Q_{10}^{(26.5-37.0)/10} = 2.78$ msec at 37° C in the animal, which explains why the NMDA current plotted in Fig. 4.9B, obtained at 23° C, has larger values of τ_1 and τ_2 than those indicated here.

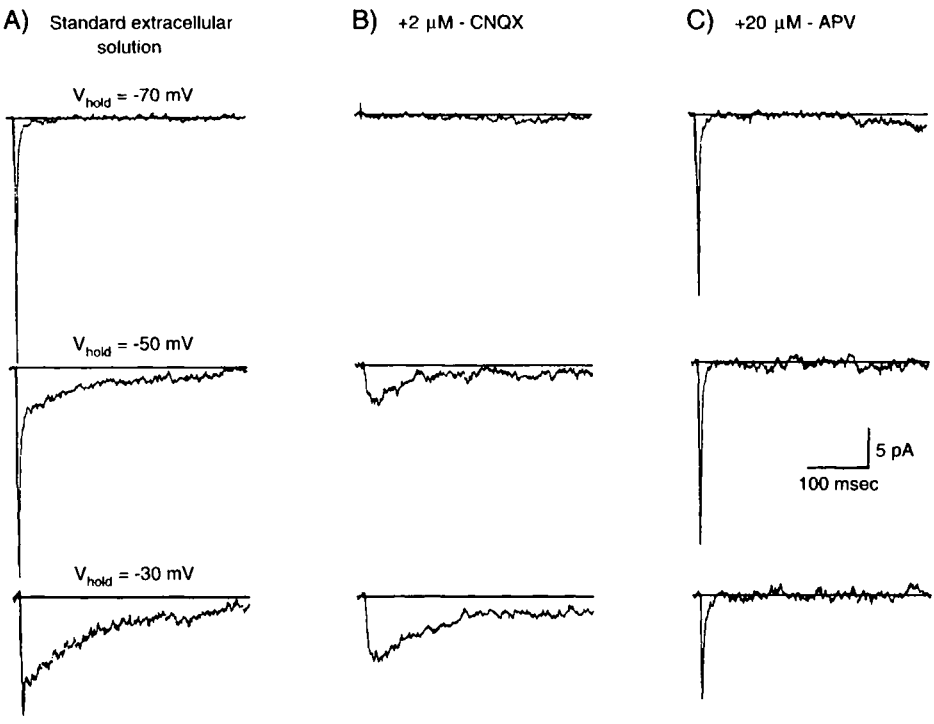

Fig. 4.9 Excitatory Postsynaptic Currents Excitatory postsynaptic current recorded at the soma of inhibitory stellate cells in slices of rat visual cortex in response to the synaptic input, recorded by clamping the membrane potential to three different values (Stern, Edwards, and Sakmann, 1992). The EPSCs are measured at three different clamp potentials. **(A)** As discussed in the text, the EPSC mainly reflects the time course of the underlying synaptic channels, while the time course of the EPSP is dictated by the electrotonic structure of the postsynaptic site. **(B)** Pharmacological dissection of the two components of a stimulus-evoked EPSC. Here, the fast component is blocked by application of the non-NMDA antagonist CNQX, while in **(C)** the slow NMDA-mediated component is blocked by APV. Because the experiments were performed at room temperatures, EPSCs in the living animal will be faster. Reprinted by permission from Stern, Edwards, and Sakmann (1992).

As discussed in Sec. 1.4, the *voltage-clamp* paradigm allows the physiologist to measure the current needed to keep the membrane at a fixed potential (the clamp potential V_{clamp}). This technique was developed by Marmont (1949), Cole (1949), and Hodgkin, Huxley, and Katz (1949) to record accurately the membrane current flowing across the axonal membrane. Using a high-gain feedback amplifier, enough current is supplied to the membrane to stabilize the potential at V_{clamp}, even if the membrane conductance is changing rapidly (as during an action potential; see Chap. 6). The basic circuit is presented in an highly idealized form in Fig. 4.10. For a primer on the theory of voltage clamping, consult Appendix A in Johnston and Wu (1995).

When voltage clamping is applied to a cell receiving synaptic input, the clamp current I_{clamp} needed to keep the membrane at V_{clamp} is usually termed *excitatory postsynaptic current* (EPSC) or *inhibitory postsynaptic current* (IPSC), depending on whether the current is negative or positive. If the synaptic input is at, or close to, the location of the electrode, cable properties can be neglected and the synaptic current can be estimated via the use of the voltage-clamp technique by fixing the somatic potential to the resting potential,

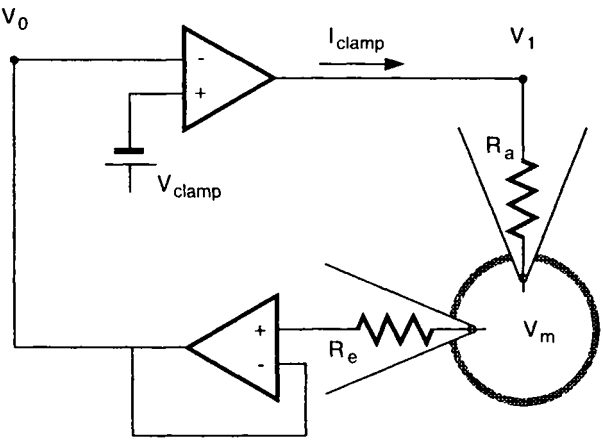

Fig. 4.10 VOLTAGE-CLAMP SETUP The technique of *clamping* the membrane potential to a particular value and measuring the resultant current constitutes a key technological advance in cellular biophysics. We here illustrate the vanilla flavored two-electrode voltage-clamp circuit schematically. The voltage recording electrode at the bottom connects to a high impedance follower circuit that acts as a buffer, drawing only minimal current from the cell. Its output voltage $V_0 \approx V_m$. This output is connected to the negative input of an amplifier with gain A. Its output voltage $V_1 = A(V_{\text{clamp}} - V_0)$. The associated current I_{clamp} flows across the access resistance R_a into or out of the cell. In the limit of a very large gain A, the membrane potential across the cell V_m is "clamped" to V_{clamp}.

$$I_{\text{clamp}}(t) = g_{\text{syn}}(t)(V_{\text{clamp}} - E_{\text{syn}}) \tag{4.7}$$

with $V_{\text{clamp}} = V_{\text{rest}}$. For synaptic inputs that only give rise to a small postsynaptic potential at the soma, the driving potential is not much changed and I_{clamp} constitutes a fair approximation to the actual postsynaptic current, defined via Eq. 4.4.

If the site of the synapse does not coincide with the site at which the membrane potential is clamped—common to most situations when one is recording from the cell body and the synaptic input is located somewhere in the dendritic tree—cable properties intervene and one no longer measures the pure synaptic current (the synapse is said to be improperly space clamped). Establishing whether or not voltage clamping is complete is a challenging problem with no cut and dry answers (see Smith et al., 1985).

In many inhibitory interneurons, excitatory input makes frequent contacts directly onto the cell bodies, allowing them to be easily voltage clamped. Stern, Edwards, and Sakmann (1992) exploit this fact to record excitatory postsynaptic currents in inhibitory stellate cells in rat visual cortex (given their small size, the associated high input resistances are very high, between 0.5 and 2 GΩ). Stimulating neighboring cells leads to the small unitary EPSCs shown in Fig. 4.9 (unitary in the sense that below a certain stimulus threshold no EPSC can be seen, while the peak amplitude of the EPSC remains constant once the threshold has been exceeded). Making judicious use of CNQX and APV, the specific blockers of the non-NMDA and the NMDA receptors, Stern and his colleagues separate the two components. Clamping the membrane to near its resting potential, it can be seen that the fast and large component is due to non-NMDA input, while the slow and late component is NMDA mediated. Clamping at progressively more depolarizing currents increases the component remaining after application of CNQX, that is, the NMDA component, while the APV-insensitive component is decreased. Because the synaptic driving potential is

progressively reduced as V_{clamp} is increased, the non-NMDA-mediated current decreases, while the NMDA current increases, the decrease in driving potential being compensated for by the increase in the conductance in the negative slope-conductance region. Glutamate-mediated synaptic input usually has both NMDA and non-NMDA components, arguing for colocalization of both receptors in the postsynaptic membrane (as in Fig. 4.9).

NMDA channels are in a sense a theoretician's dream come true, since they implement within a single protein complex a molecular AND gate: a significant depolarizing current can only be obtained in the presence of presynaptic neurotransmitters *and* postsynaptic depolarization. This action is only possible because of the fact that, different from non-NMDA excitation and GABAergic inhibition, the amplitude of the postsynaptic conductance change depends on the postsynaptic potential. NMDA receptors have been experimentally implicated as contributing toward the conjunctive nonlinearities required for Hebb's learning rule (Chap. 13).

Before finishing this section, we need to point out a crucial difference between the EPSC and the resultant EPSP (the same applies for the relationship between IPSC and IPSP): the postsynaptic current always *leads* the postsynaptic voltage. Since the current flowing across a pure capacitance is proportional to the derivative of the voltage, the voltage response to a sinuosidal current will also be sinusoidal but with a *phase shift* of 90°; the voltage lags the current by this phase angle. No such phase shift is observed for a pure resistance. For any distributed, mixed resistive and capacitive system, the current will always lead the voltage by a phase angle somewhere between 0° and 90°. While the EPSC is not equal to the current flowing during an EPSP (since in the former case the voltage is clamped to some value while it changes in the latter) it usually is similar if the voltage is clamped to the resting potential of the cell (since the voltage excursion away from V_{rest} is usually small relative to E_{syn}).

The dynamics of the current flowing at the synapse is only limited by how fast the underlying channels can switch—in the submillisecond range for fast excitatory or inhibitory input—while the evoked potential change is constrained by postsynaptic parameters (such as the intracellular resistance, the membrane capacity, and, to a much lesser extent, the membrane resistance) as discussed at length in Sec. 3.6.3.

One functional reason to stress EPSCs over EPSPs is that the *current* flowing at the soma in response to synaptic input is a much more meaningful measure of synaptic efficiency than the peak postsynaptic potential (see Chaps. 17 and 18).

4.7 Inhibitory GABAergic Synaptic Input

The most common inhibitory neurotransmitter in the central nervous system of both invertebrates and vertebrates appears to be GABA. In the thalamus and cortex, about a quarter of all cells utilize GABA. (For the recent physiological literature on GABA see McCormick, 1990; Edwards, Konnerth, and Sakmann, 1990; LaCaille, 1991; Berman, Douglas, and Martin, 1992.) The second important inhibitory neurotransmitter, glycine, appears to mediate IPSP in the spinal cord onto motoneurons (Young and MacDonald, 1983) and in the brainstem.

There are two major forms of postsynaptic receptors associated with GABA releasing terminals, termed A and B receptors. They are quite distinct from each other, with their main commonality being that they both bind GABA. As in the case for the excitatory neurotransmitters, our knowledge about these different receptor classes derives from the existence of specific blockers (antagonists): the pharmacological agents *bicuculline* and

picrotoxin reversibly block $GABA_A$ receptors while *phaclofen* blocks the B type (see Fig. 4.6).

The $GABA_A$ receptor is an ionotropic one, with binding of GABA leading to the direct opening of channels selective to chloride ions (as with the glutamate receptor, more than a dozen subreceptor types are known). The current through these channels reverses at the equilibrium potential for chloride ions, in the neighborhood of −70 mV. In many cells, only chloride conductances are open at rest, implying that their resting potential is close to E_{syn} for $GABA_A$ synapses, an important fact to which we will return. The associated postsynaptic conductance change rises very rapidly, that is, within 1 msec or less, and decays within 10–20 msec.

GABA can also bind to a metabotropic receptor, the $GABA_B$ receptor. With the help of a second messenger (a G protein), activation of this receptor type leads to the opening of channels selective to potassium ions. This makes the associated synaptic battery considerably more hyperpolarized than the reversal potential of the $GABA_A$ receptor: it is between −90 and −100 mV. Due to the indirect coupling between the release of GABA and the opening of the associated K^+ channels, the onset and the duration of the postsynaptic conductance change are much slower, with the peak not occurring until 10 msec or more after transmitter release, the total duration being on the order of 100 msec or longer.

Different from the non-NMDA and the NMDA receptors, $GABA_A$ and $GABA_B$ do not appear to be colocalized. In fact, pharmacological evidence argues for a segregation of these two receptor classes, with $GABA_A$ occurring at or close to the soma and the hyperpolarizing $GABA_B$ type farther away, out on the dendrites (Tseng and Haberly, 1988; Douglas and Martin, 1998). As we will see in the following chapter, $GABA_A$ synapses can implement a multiplication, albeit a "dirty" one, while the hyperpolarizing action of a $GABA_B$ synapse has more similarity to a linear subtraction.

4.8 Postsynaptic Potential

Section 1.4 dealt with a synapse embedded within a simple RC circuit. Let us now treat the more general case of synaptic input to some postsynaptic site i, characterized by the time-dependent input impedance $K_{ii}(t)$. The voltage change $V_i(t)$ in response to a synaptic current (Eq. 4.4) is given by Ohm's law (with all potentials relative to the resting potential and the sign of the synaptic current—following the convention of physiologists— inverted to account for the flow of electric charge),

$$V_i(t) = K_{ii}(t) * (-I_{syn}(t)) = K_{ii}(t) * \{g_{syn}(t)(E_{syn} - V_i(t))\}, \tag{4.8}$$

where $*$ represents convolution. Equation 4.8 is just a shorthand way of writing

$$\begin{aligned} V_i(t) &= \int_{-\infty}^{+\infty} K_{ii}(t - t')g_{syn}(t')(E_{syn} - V_i(t'))dt' \\ &= \int_0^t K_{ii}(t - t')g_{syn}(t')(E_{syn} - V_i(t'))dt' \end{aligned} \tag{4.9}$$

The last transformation follows from our assumption that $K_{ii}(t)$ and $g_{syn}(t)$ are zero for negative times. Equation 4.9 is a *Volterra integral equation* of the second type, characterized by the fact that the membrane potential appears both on the left-hand and on the right-hand side of the equation (Poggio and Torre, 1978).

Following Eq. 3.16, we can express the voltage at location j caused by the synaptic input at i in terms of the transfer impedance $K_{ij}(t)$,

$$V_j(t) = K_{ij}(t) * (-I_{syn}(t)) = K_{ij}(t) * \{g_{syn}(t)(E_{syn} - V_i(t))\}. \quad (4.10)$$

Because the expression for V_j depends on V_i, finding V_j necessitates the solution of a system of coupled integral equations (Eqs. 4.9 and 4.10).

4.8.1 Stationary Synaptic Input

In order to develop some intuitions about these equations, let us first treat the stationary case, that is, the case in which a fixed increase in synaptic conductance g_{syn} leads to some fixed change in the voltage. The convolution in Eqs. 4.9 and 4.10 is then reduced to a simple multiplication, and the time-dependent input impedance $K_{ii}(t)$ is replaced by the dc part of the Fourier transform, that is, by the input resistance $\tilde{K}_{ii}(f = 0) = \tilde{K}_{ii}$,

$$V_i = \tilde{K}_{ii} \cdot g_{syn}(E_{syn} - V_i) \quad (4.11)$$

or,

$$V_i = \frac{\tilde{K}_{ii} E_{syn} g_{syn}}{1 + \tilde{K}_{ii} g_{syn}}. \quad (4.12)$$

This nonlinear equation implies that the postsynaptic potential V_i does not increase indefinitely with g_{syn}, but saturates. Figure 4.11 demonstrates this in the case of transient synaptic input. The reason for the sublinear behavior is the fact that the synaptic current pushes the membrane potential toward E_{syn}, reducing the *driving potential* $E_{syn} - V_i$. As this becomes smaller, the synaptic current will also become smaller. At $E_{syn} = V_i$, the current ceases, no matter how large the conductance change, since no potential difference exists across the synaptic conductance g_{syn}.

The determinant of whether the synaptic input excites or inhibits the cell is primarily its reversal potential E_{syn}. If the battery is above the resting potential, an increase in $g_{syn}(t)$ causes an EPSP; if the converse is true, a hyperpolarizing IPSP results. In the remainder of this chapter, we only treat excitatory inputs. However, the same principles apply for inhibitory synaptic inputs.

Let us consider the membrane potential for a small synaptic input (Rinzel and Rall, 1974). "Small" is defined here relative to the input resistance. If the dimensionless product of the dc input resistance and the conductance change is much less than one, that is, $g_{syn} \cdot \tilde{K}_{ii} \ll 1$, the input is considered small. For instance, relative to a 500 MΩ dendritic input site, a 0.2 nS synaptic input is small, because $5 \times 10^8 \times 2 \times 10^{-10} = 0.1$. Under these circumstances we can approximate Eq. 4.12 by

$$V_i \approx \tilde{K}_{ii} E_{syn} g_{syn} = \tilde{K}_{ii} I_{syn}. \quad (4.13)$$

In other words, if the synaptic input is small enough, the membrane potential changes only little (that is, $E_{syn} - V_i \approx E_{syn}$), and the synaptic input can be approximated by a constant current source, $I_{syn} = E_{syn} g_{syn}$, independent of the membrane potential. If synaptic input can be treated as a current source, then doubling the amplitude of the current source will simply double the postsynaptic potential change, no bothersome saturating behavior exists, and the output is linear in the input.

We discussed in Secs. 4.6 and 4.7 evidence for conductance increases at single glutamate and GABA synapses of 1 nS or less. This implies that as long as the postsynaptic site has

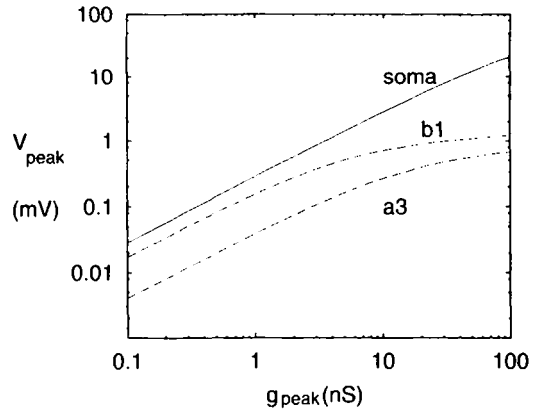

Fig. 4.11 SYNAPTIC SATURATION Relationship between the postsynaptic conductance change and the peak somatic EPSP on a log-log plot. A single fast ($t_{peak} = 0.5$ msec) synapse of variable amplitude g_{peak} is activated at one of three different locations—the soma and at two dendritic sites ($a3$ and $b1$; Fig. 3.7)—and the peak somatic EPSP is shown. Given the relatively high input conductance at the cell body, the somatic input does not saturate within the range shown here, while the two dendritic synapses are saturating for inputs above 10 nS. The simultaneous or near-simultaneous activation of many synapses can easily increase the membrane conductance by this amount or more. Synaptic saturation has important consequences for the cell during massive synaptic input. $R_m = 20,000\ \Omega \cdot \text{cm}^2$, $V_{rest} = -65$ mV and $E_{syn} = 0$ mV.

an input resistance of less than several hundred megaohms, individual inputs can be treated as current injection. This is frequently the case for cortical pyramidal cells, where a single synaptic input can often be treated as a current source. Only in the distal dendrites and thin and elongated spines will the "current" approximation be invalid. However, in the presence of massive synaptic input, as would occur under physiological conditions when hundreds of inputs can be active simultaneously, saturation occurs and has important functional consequences (Chap. 18).

If the product of g_{syn} and $\tilde{K}_{ii}$ becomes larger, but still less than 1, we can use the Taylor series expansion of $1/(1+x) = 1-x+x^2+O(x^3)$ and express the postsynaptic potential as

$$V_i = g_{syn}\tilde{K}_{ii}E_{syn}\left[1 - g_{syn}\tilde{K}_{ii} + (g_{syn}\tilde{K}_{ii})^2 + O((g_{syn}\tilde{K}_{ii})^3)\right] \qquad (4.14)$$

where $O((\ldots)^3)$ is a shorthand notation for cubic and higher order terms. Intuitively, we can think of this series expansion in terms of adding higher order correction terms to the linear current term: first the synapse opens and the current $I_{syn} = E_{syn}g_{syn}$ flows into the cell, causing a change in membrane potential (given by $\tilde{K}_{ii}E_{syn}g_{syn}$; see Eq. 4.13). This variation in membrane potential changes in turn the driving potential from E_{syn} to $E_{syn}(1 - g_{syn}\tilde{K}_{ii})$, which will decrease the potential by $E_{syn}(g_{syn}\tilde{K}_{ii})^2$, which again leads to a change in the driving potential, and so on. Adding up all these terms leads to the above equation. Effectively, we approximate the conductance input g_{syn} by a current input plus a number of "correction" terms: $V_i = \tilde{K}_{ii}(I_{syn}^{(1)} + I_{syn}^{(2)} + I_{syn}^{(3)} + \cdots)$.

In the other extreme case, when the product of the synaptic conductance change and the input resistance is very large, that is, $g_{syn}\tilde{K}_{ii} \gg 1$, we have

$$V_i \approx E_{syn}\,. \qquad (4.15)$$

The synapse is saturated (Fig. 4.11). As we have seen already in Fig. 1.11 and will discuss further on in more detail, this nonlinear behavior of synapses can be exploited

to implement a number of nonlinear neuronal operations, in particular multiplication. The nonlinear transduction process between conductance change and membrane potential was fully recognized by Rall (1964), although usually disregarded by him and other early modelers, both because the nonlinearity involved usually precludes analytical treatment and because the input resistance in the dendritic tree was thought to be relatively small.

The steady-state potential at any other location j in response to a constant synaptic input at location i (Eq. 4.10) is given by

$$V_j = \tilde{K}_{ij} I_{\text{syn}} = \tilde{K}_{ij} \frac{V_i}{\tilde{K}_{ii}} = \frac{\tilde{K}_{ij} E_{\text{syn}} g_{\text{syn}}}{1 + \tilde{K}_{ii} g_{\text{syn}}}. \tag{4.16}$$

The denominator of this expression is identical to the one describing the potential at location i (Eq. 4.12). Therefore, the saturation behavior (e.g., whether or not the synaptic input can be treated as a current) only depends on the electrical properties at the synapse i and not on the transfer resistance $\tilde{K}_{ij}$. Indeed, the potential at j is given by the voltage at i divided by the voltage attenuation,

$$V_j = \frac{V_i}{A^v_{ij}} \tag{4.17}$$

4.8.2 Transient Synaptic Input

In the previous section, we assumed for the sake of mathematical convenience that the synaptic input is so slow that it can be treated as a sustained dc input. Under most physiological conditions, though, fast excitatory synaptic input is anything but stationary but can be over in a time interval less than τ_m.

Solving analytically for the voltage in response to transient conductance inputs is difficult. Numerical evaluations can be carried out in one of two different manners. Either one can first compute the appropriate input and transfer impedances using the cable equation and then solve Eqs. 4.8 and 4.10, or one can directly integrate the cable equation. The first method suffers from the disadvantage that computing the potential in response to n spatially distributed inputs requires the evaluation of about $n^2/2$ input and transfer impedances and only works for a linear membrane, while the second method does not depend on the number of inputs and can be extended in a straightforward manner to deal with membrane nonlinearities.

For a single synaptic input $g_{\text{syn}}(t)$ at location x_0 onto a single passive dendrite, the modified cable equation (Eq. 2.7) has the form

$$\lambda \frac{\partial^2 V_m(x,t)}{\partial x^2} = \tau_m \frac{\partial V_m(x,t)}{\partial t} + V(x,t) + \delta(x_0) r_m g_{\text{syn}}(t)(V_m(x,t) - E_{\text{syn}}) \tag{4.18}$$

with the appropriate boundary conditions.

Historically, it was Rall and his collaborators who first studied solutions to this equation for a variety of different dendritic tree geometries (Rall and Rinzel, 1973; Rinzel and Rall, 1974; Segev et al., 1985). This equation is difficult to solve in closed form and we will not attempt to do so. Rather, the course we follow throughout the book is to integrate the cable equation numerically. Because of their generality, simple numerical integration algorithms are the methods of choice today for solving these partial differential equations (see Appendix C). We made use of the very efficient and freely distributed single-cell simulator program package called NEURON for generating most of the figures in this book. NEURON was developed by Hines (1984, 1989, 1998) and is widely used in the

computational neuroscience community. An even more powerful tool is the single cell and neuronal network simulation package GENESIS, developed by Bower and his group (DeSchutter, 1992; Bower and Beeman, 1998).

Figure 4.12 shows the dendritic and somatic EPSPs due to a single non-NMDA excitatory synaptic input located in the basal tree of our layer 5 pyramidal cell. Notice the small size of the somatic EPSP, requiring summation of many excitatory inputs before the membrane potential reaches the firing threshold. If the same input is located at more distal locations (not shown; see, however, Fig. 18.1), the somatic EPSP is even smaller and its peak occurs later in time. Rall has derived in the case of a single equivalent cylinder a relationship between the time of peak potential and the location of synaptic input (Rall et al., 1967), which has been used to infer synaptic location in the case of *Ia* synaptic input to α motoneurons (Smith, Wuerker, and Frank, 1967). Because pyramidal cells do not fulfill the conditions for reduction to an equivalent cable (Sec. 3.2), no simple analytical relationship between time to peak and location exists. Furthermore, because of the low-pass action of the dendritic tree, the peak potential becomes more and more smeared out as the synaptic input moves away from the soma, making the time at which the peak potential occurs more and more difficult to define.

4.8.3 Infinitely Fast Synaptic Input

What occurs when we consider the other extreme, that of a conductance change that occurs infinitely fast or, in practice, much faster than the neuronal time constant τ_m? Because the conductance change is so rapid, it does not have time to change the membrane potential,

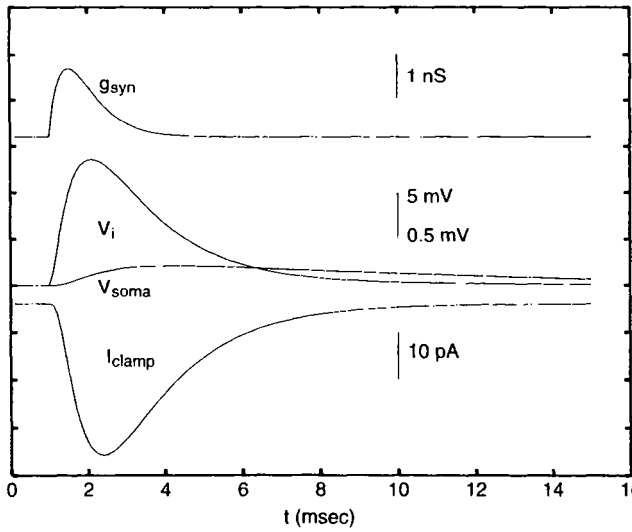

Fig. 4.12 EXCITATORY SYNAPTIC INPUT Simulated synaptic input in response to activation of a single, fast non-NMDA excitatory input in the basal tree of our pyramidal cell (at location *b*1 in Fig. 3.7). We here show the synaptic conductance change $g_{syn}(t)$ (activated at 1 msec and peaking 0.5 msec later) and the local as well as the somatic EPSP (the 5-mV scale bar applies to V_i, while the 0.5-mV scale applies to V_{soma}). Notice the small amplitude of the somatic EPSP, in agreement with experiments (Fig. 4.4). The bottom trace shows the clamp current in response to this input, when the soma is clamped to −65 mV. This approximates the current at the soma when the synaptic input is activated.

and therefore the driving potential, appreciably before it is over. Thus, we expect a very fast conductance input to act like a current input. This can be shown quite easily by assuming $g_{syn}(t) = g_{peak}\delta(t)$. Replacing this into the convolution Eq. 4.9 yields

$$V_i(t) = g_{peak}\int_{-\infty}^{+\infty} K_{ii}(t-t')\delta(t')(E_{syn} - V_i(t'))dt' = g_{peak}K_{ii}(t)E_{syn} \quad (4.19)$$

assuming that $V_i(t = 0) = 0$ (relative to V_{rest}). The resulting EPSP faithfully follows the impulse response function $K_{ii}(t)$. From this we expect that very fast synaptic inputs will show little evidence of conductance changes, even if they are large.

4.9 Visibility of Synaptic Inputs

A question of experimental interest is to what extent a synaptic conductance change can be detected at the cell body using an intracellular electrode. This issue is of paramount concern when trying to resolve the question of the existence and strength of conductance changes, in particular those associated with inhibition, during visual stimulation of neurons in both retinal ganglion cells (Marchiafava, 1979; Watanabe and Murakami, 1984) and cortical neurons (Douglas, Martin, and Whitteridge, 1988; Pei et al., 1991; Ferster and Jagadeesh, 1992; Borg-Graham, Monier, and Frégnac, 1998).

It has been proposed that shunting or silent inhibition vetoes the response of the cell when the visual stimulus, usually a spot or bar of light, moves in the cell's null direction (Torre and Poggio, 1978; Koch, Poggio, and Torre, 1982; Koch and Poggio, 1985b; Sec. 5.1). These theoretical ideas can be tested experimentally by inferring the existence of synaptically mediated shunting inhibition, raising the general issue of the conditions under which a synaptic input somewhere in the dendritic tree can be seen by an electrode at the cell body (Rall, 1967).

One problem is that an intracellular electrode cannot record conductance inputs directly; rather they have to be inferred from their shunting effect on the voltage. A sustained conductance change is measured by injecting a steady-state current I_s at the soma and recording the resultant stationary voltage V_s; the ratio of these two corresponds to the input conductance $\tilde{G}_{ss} = 1/\tilde{K}_{ss}$. The same procedure is repeated during synaptic stimulation. The difference between the old and the new values of the somatic input conductance then corresponds to the change in input conductance $\Delta\tilde{G}_{ss}$ due to the synaptic input g_{syn}. The voltage at the postsynaptic site i is the sum of the synaptic contribution and the current spread from the somatic current injection,

$$V_i = g_{syn}\tilde{K}_{ii}(E_{syn} - V_i) + \tilde{K}_{is}I_s\,. \quad (4.20)$$

The somatic EPSP in the presence of both synaptic input and injected current is

$$V_s' = g_{syn}\tilde{K}_{is}(E_{syn} - V_i) + \tilde{K}_{ss}I_s\,. \quad (4.21)$$

It is now straightforward to show (Koch, Douglas, and Wehmeier, 1990) that the change in somatic input resistance ΔK_{ss} is given by

$$\Delta\tilde{K}_{ss} = \frac{-g_{syn}\tilde{K}_{is}^2}{1 + g_{syn}\tilde{K}_{ii}}\,. \quad (4.22)$$

As expected for any input with $g_{syn} \geq 0$, $\Delta\tilde{K}_{ss}$ is always negative; physically, this corresponds to the input resistance decreasing in response to an increase in the membrane

conductance. Furthermore, it can be proven that the change in input conductance $\Delta\tilde{G}_{ss}$ is always bound by the total synaptic change, that is, $0 \leq \Delta\tilde{G}_{ss} \leq g_{\text{syn}}$.

The equation itself is simple to understand. The current injected at the soma I_s induces a voltage change $\tilde{K}_{is}I_s$ at the location of the synapse. This voltage provides a synaptic driving force, which converts the synaptic conductance input g_{syn} into a voltage change at location i, that is, $(\tilde{K}_{is}I_s)\tilde{K}_{ii}g_{\text{syn}}/(1 + g_{\text{syn}}\tilde{K}_{ii})$. This is propagated to the soma, causing a voltage change $g_{\text{syn}}\tilde{K}_{is}^2 I_s/(1 + g_{\text{syn}}\tilde{K}_{ii})$. Dividing this voltage by the current I_s leaves the resistance change.

The higher the input resistance $\tilde{K}_{ii}$ at the synapse, or the further removed the synapse is from the cell body ($\tilde{K}_{is} \to 0$), the less visible the synaptic input becomes. Even if the synaptic conductance change is very large, its effect on the soma will always be limited (as $g_{\text{syn}} \to \infty$, the change in input resistance will converge to $-\tilde{K}_{is}^2/\tilde{K}_{ii}$), except if the input is located directly at the soma, since in that case $\Delta\tilde{K}_{ss} \to -\tilde{K}_{ss}$ and the new input conductance goes to zero.

Notice that $\Delta\tilde{K}_{ss}$ does not depend on the synaptic battery. In principle, this implies that hyperpolarizing, shunting, or excitatory synaptic inputs are all equally visible from the recording electrode. Due to the capacitive nature of the neuronal membrane, transient conductance changes are more difficult to see from the soma than sustained ones (since additional charge between the synapse and the soma flows onto the distributed capacitances). Therefore, Eq. 4.22 represents an upper bound on what can be seen of a conductance change at the cell body.

4.9.1 Input Impedance in the Presence of Synaptic Input

In the previous chapter, we defined the input impedance in a quiescent system without any synaptic input. If a sustained synaptic input occurs at i, the new value of the somatic input resistance

$$\tilde{K}'_{ss} = \tilde{K}_{ss} + \Delta\tilde{K}_{ss} \tag{4.23}$$

follows simply from Eq. 4.22.

In the presence of a time-dependent conductance change, the system is a nonstationary one and the new input conductance is not simply the sum of the time-varying conductance change $g_{\text{syn}}(t)$ and the old conductance change. In the case of a patch of membrane without spatial extent characterized by the input impedance $K(t)$, the new input impedance $K'(t, t')$ is a two-dimensional function depending on the time the synaptic input arrived,

$$\frac{1}{K'(t, t')} = g_{\text{syn}}(t) + \frac{1}{K(t' - t)}. \tag{4.24}$$

The exact value of the conductance change depends on the relative timing between the onset of the synaptic input and the onset of the current pulse used to measure the input impedance. For stationary input, we obtain the familiar $1/K' = g_{\text{syn}} + 1/K$.

4.10 Electrical Gap Junctions

As we mentioned, neurons are also coupled using direct electrical connections (Dermietzel and Spray, 1993). This point-to-point coupling occurs at specialized channels spanning the pre- and postsynaptic membranes called *gap junctions*. Such a junction provides a

direct, high-conductance pathway between between neurons and eliminates the possibility that the gap junction current would be shunted by the extracellular space. The strength of the coupling can be modulated by a number of factors, such as high internal calcium concentration (a feature thought to protect the surrounding tissue from the death of any one cell) or intracellular pH (Bennett and Spray, 1987).

Many cells are coupled by gap junctions, giving rise to a *syncytium* of two- or three-dimensional cellular networks. The most dramatic example is the cardiac muscle. Gap junctions allow single action potentials, originating in a group of pacemaker cells, to sweep through all cells in a wavelike manner, generating the rhythmic squeeze and relaxation that is the stuff of life (Noble, 1979).

Glial cells are another example. These cells, thought to play mainly a supporting, metabolic role in the nervous system—such as maintaining the ionic distributions and gradients necessary to homeostasis—lack conventional chemical synapses. They communicate instead via an extensive grid of electrical gap junctions with each other (Giaume and McCarthy, 1996).

One way to study gap junctions is to record from two coupled cells using pipettes, and measuring the current flow between the two as a function of the voltage gradient (Fig. 4.13A). In general, one observes a linear I–V curve, whose slope depends on the number of gap junction channels among the pair of cells (Fig. 4.13B). Typically, each channel contributes about 100 pS of conductance. Gap junctions are usually symmetrical, with a depolarization in one cell leading to a depolarization in the other one, albeit of less value, and a hyperpolarization leading to a less pronounced hyperpolarization in the other cell. From an electrical point of view, this situation can be mimicked by postulating a coupling conductance g_c among the two cells (Fig. 4.13C).

When current is injected into cell 1, as shown in the figure, the application of Kirchhoff's current law to the two nodes and the neglect of all transient behavior leads to the following expression for the transfer resistance:

$$\tilde{K}_{12} = \frac{g_c}{g_1 g_2 + g_1 g_c + g_2 g_c} = \tilde{K}_{21}\,, \tag{4.25}$$

where g_1 and g_2 correspond to the input conductance of each cell. The inverse of the slope of the I–V curve in Fig. 4.13B corresponds to this coupling resistance. The input resistance of cell 1 is

$$\tilde{K}_{11} = \frac{g_c + g_2}{g_1 g_2 + g_1 g_c + g_2 g_c}\,. \tag{4.26}$$

Equation 4.25 implies that injecting some current into cell 1 induces the same voltage in cell 2 as injecting the current in cell 2 and measuring the voltage in cell 1. In order to see the asymmetry inherent in direct electrical coupling, we compute the voltage attenuation experienced by going from cell 1 to cell 2,

$$A_{12}^{v} = \frac{g_2 + g_c}{g_c} \tag{4.27}$$

and in the opposite direction,

$$A_{21}^{v} = \frac{g_1 + g_c}{g_c} \tag{4.28}$$

Let us assume a coupling conductance of $g_c = 1$ nS and an input conductance of $g_2 = 10$ nS for the second cell. If the first cell has the same input conductance, $A_{12}^{v} = A_{21}^{v} = 1.1$, that

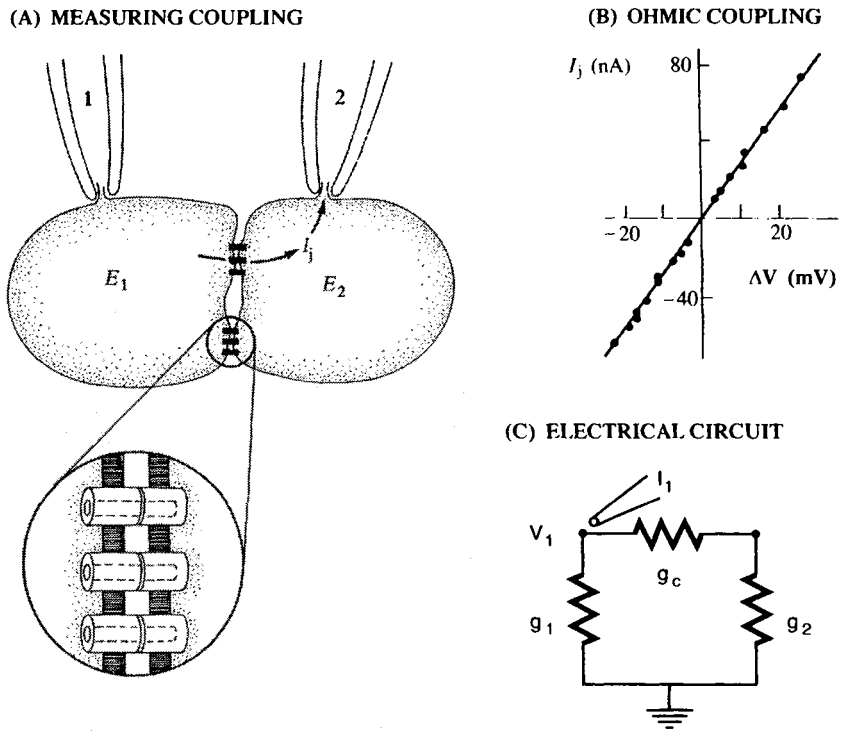

Fig. 4.13 ELECTRICAL COUPLING A second type of specific cell-to-cell coupling occurs via *gap junctions* or *electrical synapses*. **(A)** They can be studied by applying a membrane potential across two adjacent cells and measuring the junctional current. Different from a chemical synapse, the current flows instantaneously, with no delay. The inset provides a graphical rendition of the molecular nature of the voltage-independent channels underlying this coupling. Reprinted by permission from Hille (1992). **(B)** The resultant I–V curve, here taken from the gap junction among axons in the crayfish motor system (Watanabe and Grundfest, 1961). The inverse of the slope corresponds to the transfer resistance $\tilde{K}_{12}$ of Eq. 4.25. **(C)** The majority of such junctions can be modeled by a coupling conductance g_c. Current flows from one cell to the next without being shunted by the extracellular cytoplasm. The capacitive nature of the pre- and postsynaptic membranes has been neglected.

is, an EPSP would be attenuated by about 10% in either direction. However, if cell 1 is much smaller, with a tenfold lower conductance of $g_1 = 1$ nS, then the voltage attenuates by a factor of 2 when going from the low-input to the high-input conductance cell, while it still only attenuates by 10% in the opposite direction. Attenuation is symmetrical when the two input conductances g_1 and g_2 are identical. It should be pointed out that attenuation across an electrical synapse is in marked contrast to the high degree of amplification possible at chemical synapses.

Electrical coupling has been studied in detail in the outer layers of the vertebrate retina. Gap junctions among rods as well as among horizontal cells give rise to extended two-dimensional sheets of cells (Kaneko, 1976; Copenhagen and Owen, 1976; Attwell and Wilson, 1980). Theoretical calculations show that a spatio-temporal filter can be ascribed to this syncytium (Torre, Owen, and Sandini, 1983; Torre and Owen, 1983). Indeed, the experimental data suggest that the high-pass filtering properties of the rod network serve to optimize the signal-to-noise ratio by integrating visually evoked signals over a large area

for rapid signals and over a small area for slowly changing ones (Detwiler, Hodgkin, and McNaughton, 1980).

In the adult thalamus and cortex, gap junctions have only occasionally been reported. At this point in time it is safe to say that the mere existence as well as any possible functional role of electrical synapses in cortex and associated structures remain unknown.

Electrical synapses do not have any intrinsic delay, unlike chemical ones. Thus, one frequently finds them in time-critical pathways. The classical example is electrical synapses made by presynaptic fibers onto axons of giant motor neurons that mediate the emergency tail flips in the crayfish, the basis of its escape reaction during danger (Furshpan and Potter, 1959). Interestingly, here the connection is rectifying, with a diode-like relationship between the voltage across and the current flowing through this junction.

A further example is the part of the electrosensory system in weakly electric fish that conveys information about the time of occurrence of the zero crossing of the electrical wave signal that the fish can send out and also sense (Heiligenberg, 1991). At multiple locations in this pathway, electric synapses mediate cell-to-cell coupling. For instance, spikes in the so-called T afferents from the periphery carry temporal information in action potentials with a time jitter of 30 ± 25 μsec. A number of these afferents make gap junctions with a spherical cell in the *electrosensory lateral line lobe*, such that a randomly occurring input in any one input fiber does not bring the cell to threshold. Using this conjunctive logic together with synapses that do not introduce any additional temporal smear, reduces the temporal jitter of the output spikes to 11 ± 3 μsec (Carr, Heiligenberg, and Rose, 1986).

One functional role of gap junctions most certainly has to do with the fact that small molecules, such as cAMP (or intracellular dye in an experiment), can pass through these channels, enabling them to diffuse across many cells. This might explain the more widespread distribution of gap junctions during early development (DeHaan and Chen, 1990).

4.11 Recapitulation

Fast communication among nerve cells occurs at specialized junctions called synapses. They are very compact: between several hundred million and one billion synapses can be packed into one cubic millimeter of neuronal tissue. Of the two types, chemical and electrical, we focus on the former since they are much more frequent and make very specific point-to-point connections.

It is useful to distinguish fast ionotropic chemical synapses, acting on a millisecond time scale, from metabotropic chemical synapses, acting on a time scale of a fraction of a second to minutes. Conceptually and *cum grano salis*, ionotropic synapses are of the essence in the rapid forms of neuronal communication and computations underlying perception and motor control.

In response to a presynaptic change in membrane potential at a synapse, neurotransmitters are released and diffuses within a fraction of a millisecond across the cleft separating pre- and postsynaptic terminal. At the postsynaptic terminal, neurotransmitter molecules bind to specific receptors, which usually—either directly or indirectly, via involvement of a second-messenger system—open specific ionic channels. Depending on the neurotransmitter-receptor kinetics, these channels remain open for some time and a synaptic current flows across the membrane. Synaptic transmission at central synapses appears to be stochastic. A presynaptic action potential has a probability p of causing a release of a vesicle and a postsynaptic response, where p can be as small as a few percent and depends on the spiking

history of the synapse. The amplitude of the postsynaptic signal is variable as well. These factors need to be taken into consideration when thinking about neural computation.

An electrical engineer would be justified in treating a chemical synapse (at the time scale of tens of milliseconds) as a nonreciprocal, two-port device (see the introduction to Sec. 3.4). A two-port description is necessary, since a pair of equations (for both the pre- and the postsynaptic current and voltage changes) is required to completely characterize its behavior; it is non-reciprocal since changes at the postsynaptic side have no (fast) effect on the presynaptic side. Synapses serve to decouple neuronal elements that can each have very different electrical impedances, rather like a follower-amplifier circuit.

At the macroscopic and phenomenological level, a fast synaptic input induces a time-dependent increase in conductance $g_{\text{syn}}(t)$ in series with a battery E_{syn}. The sign of E_{syn} relative to the membrane potential at the postsynaptic terminal determines whether synaptic input causes an EPSP (excitatory synapse), an IPSP (inhibitory synapse), or no change in membrane potential (silent or shunting inhibition). The five dominant types of fast synaptic inputs are (1) non-NMDA or AMPA voltage-independent excitation; (2) ACh-mediated excitation; (3) the voltage-dependent and slower NMDA excitatory input that is thought to be crucially involved in synaptic plasticity; (4) the GABA_A type of silent inhibition; and (5) the slower GABA_B hyperpolarizing inhibition. The fact that synaptic input increases the postsynaptic membrane conductance in series with a battery has important consequences. In particular, synaptic inputs can saturate, will influence the input conductance of the cell, and can interact with each other nonlinearly. Only if the amplitude of the synaptic input conductance change is small relative to the local input impedance can synaptic input be treated as a constant current source.

The immense variety of neurotransmitters and postsynaptic receptors gives rise to a staggering combination of possible pairings that act on all possible time scales, and across different spatial scales, from a single synapse to a single ganglion or an entire neural system, such as the thalamus. Synapses are responsible for the most salient difference between nervous systems and even our most advanced digital computers: while the former adapt and learn—a subject we will cover in depth in Chap. 13—the latter do not.

Electrical synapses allow for direct current flow among adjacent neurons. A gap junction can usually be modeled by a fixed conductance. Different from chemical synapses where amplification between the pre- and postsynaptic sites can occur, here the signal is always attenuated. One advantage of this mode of cellular communication is speed, since no synaptic delay occurs. Thus, electrical synapses are frequently found in neuronal pathways, which subserve information that needs to be communicated very rapidly and faithfully. In the retina, gap junctions among photoreceptors and horizontal cells create vast, electrically interconnected networks that filter the incoming visual signal.